Fisheries and Oceans Canada
Pêches et Océans Canada

Ecosystems and Oceans Science
Sciences des écosystèmes et des océans

Canadian Science Advisory Secretariat (CSAS)

Research Document 2017/007

Pacific Region

Assessing the risk of lethal ship strikes to humpback (*Megaptera novaeangliae*) and fin (*Balaenoptera physalus*) whales off the west coast of Vancouver Island, Canada

Linda M. Nichol[1], Brianna M. Wright[1], Patrick O'Hara[2,3], John K.B. Ford[1]

[1]Pacific Biological Station
Fisheries and Oceans Canada
3190 Hammond Bay Road
Nanaimo, BC V9T 6N7

[2]Institute of Ocean Sciences
Canadian Wildlife Service
Environment Canada
9860 West Saanich Road
P.O. Box 6000
Sidney, BC V8L 4B2

[3]University of Victoria
Department of Biology
P.O. Box 3020 Station CSC
Victoria, BC V8W 3N5

July 2017

Foreword

This series documents the scientific basis for the evaluation of aquatic resources and ecosystems in Canada. As such, it addresses the issues of the day in the time frames required and the documents it contains are not intended as definitive statements on the subjects addressed but rather as progress reports on ongoing investigations.

Research documents are produced in the official language in which they are provided to the Secretariat.

Published by:

Fisheries and Oceans Canada
Canadian Science Advisory Secretariat
200 Kent Street
Ottawa ON K1A 0E6

http://www.dfo-mpo.gc.ca/csas-sccs/
csas-sccs@dfo-mpo.gc.ca

ISSN 1919-5044

Correct citation for this publication:

Nichol, L.M., Wright, B.M., O'Hara, P., and Ford, J.K.B. 2017. Assessing the risk of lethal ship strikes to humpback (*Megaptera novaeangliae*) and fin (*Balaenoptera physalus*) whales off the west coast of Vancouver Island, Canada. DFO Can. Sci. Advis. Sec. Res. Doc. 2017/007. vii + 33 p.

TABLE OF CONTENTS

LIST OF TABLES

LIST OF FIGURES

ABSTRACT

Vessel strikes are a source of mortality and injury for baleen whales that can have population-level impacts. Spatial analysis of whale distributions and marine traffic provide a valuable approach for identifying zones of high relative collision risk. We conducted 34 systematic aerial surveys (2012-2015) in fall and winter to estimate humpback and fin whale densities off the west coast of Vancouver Island, Canada. This region includes approaches to major shipping lanes in Juan de Fuca Strait, a gateway to the ports of southern British Columbia and Puget Sound, Washington. To predict whale densities (per km^2) in the study area, we fit negative binomial Generalized Additive Models (GAMs) to whale sightings data, incorporating survey effort as an offset and depth (m), slope (deg) and latitude (northing, UTM) as environmental covariates. Humpbacks were primarily observed on the continental shelf, with highest predicted densities along the beginning of the shelf edge (~200 m), whereas fin whales were largely predicted to occur west of the shelf in deeper water (>450 m).

We then mapped AIS-reported ship traffic densities (2013) over the same study area and combined these data with the GAM-predicted whale densities to estimate the relative risk of whale-ship collisions. Since vessel speed is an important determinant of collision lethality, we also calculated the relative risk of lethal injuries, given the probability that a strike occurs. Humpbacks were most likely to be struck along the shelf edge, the inshore approaches to Juan de Fuca Strait, and within the western portion of strait itself. Fin whales were most likely to be struck in the offshore approaches to Juan de Fuca Strait and inside the western portion of strait. Ship traffic is predicted to increase as a result of port expansions and developments in both BC and Washington State. We therefore tested future shipping projections from two sources and incorporated these predicted increases in ship traffic into our models to estimate the change in relative risk of ship strike and lethal ship strike by 2030. Our study is the first to assess ship strike risk to large whales off the west coast of Vancouver Island. The estimates of strike probability and risk of lethal strike we present here are minimum estimates, as our models did not account for species specific vulnerabilities and future projections did not account for whale population growth or anticipated increases in ship size.

Évaluer le risque de collisions mortelles avec des navires pour le rorqual à bosse (*Megaptera novaeangliae*) et le rorqual commun (*Balaenoptera physalus*) au large de la côte ouest de l'île de Vancouver, au Canada

RÉSUMÉ

Les collisions avec des navires sont une source de mortalité et de blessures qui peuvent avoir des répercussions au niveau de la population chez les mysticètes. Une analyse spatiale de la répartition des baleines en comparaison avec le trafic maritime est une méthode précieuse pour déterminer les zones où les risques relatifs de collision sont élevés. Nous avons effectué 34 relevés aériens systématiques (2012-2015) en automne et en hiver pour évaluer les densités de rorqual à bosse et de rorqual commun au large de la côte ouest de l'île de Vancouver, au Canada. Cette région comprend les approches des voies de navigation principales dans le détroit de Juan de Fuca, un accès aux ports du sud de la Colombie-Britannique et de la baie Puget dans l'État de Washington. Pour prévoir la densité des rorquals (par km^2) dans la zone d'étude, nous avons appliqué des modèles additifs généralisés (GAM) utilisant une distribution de l'erreur binomiale négative aux données d'observation des baleines, en y intégrant les efforts de relevé à titre de compensation ainsi que la profondeur (m), la pente (degrés) et la latitude (ordonnée, MTU) à titre de covariables environnementales. Les rorquals à bosse ont surtout été observés sur le plateau continental, les prévisions de densité les plus élevées se trouvant le long du début de la bordure de plateau (environ 200 m). En ce qui concerne les rorquals communs, les prévisions les situaient en grande partie à l'ouest du plateau continental, dans les eaux plus profondes (plus de 450 m).

Nous avons ensuite cartographié les densités du trafic maritime (2013) tirées du système d'identification automatique (SIA) sur la même zone d'étude, puis nous avons combiné ces données aux densités de rorquals prédites à l'aide des GAM pour estimer le risque relatif de collisions entre les rorquals et les navires. Étant donné que la vitesse des navires est un facteur déterminant et important de la létalité des collisions, nous avons aussi calculé le risque relatif de blessures mortelles, compte tenu de la probabilité qu'une collision se produise. Selon les résultats, c'est le long du bord du plateau, dans les approches côtières du détroit de Juan de Fuca et dans la partie ouest du détroit à proprement parler que les collisions sont les plus probables entre des navires et des rorquals à bosse. Pour les rorquals communs, le risque de collision avec des navires est le plus grand dans les approches extracôtières du détroit de Juan de Fuca et dans la partie ouest de celui-ci. Le trafic maritime devrait augmenter en raison des agrandissements des ports et des projets d'aménagement en Colombie-Britannique et dans l'État de Washington. Nous avons donc mis à l'essai les prévisions de navigation maritime qui provenaient de deux sources et nous avons intégré ces hausses prévues de la circulation maritime dans nos modèles en vue d'évaluer le changement du risque relatif de collisions avec des navires et de collisions mortelles avec des navires d'ici 2030. Notre étude est la première à évaluer le risque de collision avec des navires pour les grandes baleines au large de la côte ouest de l'île de Vancouver. Les calculs de la probabilité de collision et du risque de collisions mortelles que nous présentons ici ne sont que des estimations minimales, puisque nos modèles ne tiennent pas compte des vulnérabilités propres à chaque espèce. De plus, les projections pour l'avenir n'ont pas pris compte de la croissance de la population de baleines ou des augmentations prévues de la taille des navires.

INTRODUCTION

Vessel strikes, or collisions between ships and cetaceans, have been identified as a key threat to the recovery of baleen whale populations in Canadian Pacific waters (Fisheries and Oceans Canada 2013a, 2013b). Populations of baleen whales that are vulnerable to ship strikes in British Columbia include humpback whales (*Megaptera novaeangliae*), fin whales (*Balaenoptera physalus*), blue whales (*Balaenoptera musculus*), North Pacific right whales (*Eubalaena japonica*), and sei whales (*Balaenoptera borealis*), which are designated by the Committee on the Status of Endangered Wildlife in Canada as ‘Special Concern’, ‘Threatened’, ‘Endangered’, ‘Endangered’ and ‘Threatened’, respectively (COSEWIC 2015). Baleen whales are at greater risk of being struck by ships than other marine mammals because of their large body size and limited ability to manoeuvre away from oncoming vessels (Silber et al. 2010, McKenna et al. 2015). Furthermore, these species often spend extended periods of time at or near the surface, either feeding (Kot et al. 2014, Constantine et al. 2015) or recovering from the energetic demands of lunge-feeding at depth (Acevedo-Guitierrez et al. 2002, Goldbogen et al. 2006), which makes them more vulnerable to vessel strikes (Laist et al. 2001). Ship strike risk to baleen whales is even higher at night, both because ship operators cannot visually detect whales (Webb & Gende 2015), and because planktonic prey migrate toward the surface at dusk (Croxall et al. 1985), resulting in shallower feeding dives (Croll et al. 1998, Oleson et al. 2007, Calambokidis et al. 2008a, Nowacek et al. 2011). Blue whales are also known to transition to even shallower (16 ± 9.6 m; S.D.) resting dives at night (Oleson et al. 2007, Calambokidis et al. 2008a), when feeding presumably ceases because krill have dispersed to the extent that foraging is no longer profitable. These diel shifts in dive behaviour, which are typical of most baleen whales, place them within the draft depths of oncoming vessels (Constantine et al. 2015). Many large cargo ships and tankers have hulls reaching depths of 8-18 m (Silber et al. 2010, Herbert Engineering Corp. and Environmental Research Consulting 2014, Constantine et al. 2015), and due to the hydrodynamic forces around a moving ship, the lethal strike zone can extend 1-2 times beyond a ship’s actual draft (Silber et al. 2010).

Unfortunately, most baleen whales exhibit limited abilities to react to close-approaching vessels, or do not attempt to avoid ships at all. For instance, although blue whales are able to dive in response to nearby ships, they do not appear to use directed lateral movements to avoid being struck (McKenna et al. 2015). Harris et al. (2012) report a large variation in the responsiveness of humpback whales to cruise ships in Southeast Alaska; some whales did not react at all and seemed unaware of ships even during close approaches, while others displayed last-second flight responses. North Atlantic right whales (*Eubalaena glacialis*) similarly do not respond to the sounds of approaching ships (either real or played-back recordings) (Nowacek et al. 2004). This lack of avoidance behaviour may be caused by habituation to vessel noise (Nowacek et al. 2004), failure to perceive the vessel as a potential threat, or unwillingness to cease important activities such as feeding or mating (Silber et al. 2010). Fin whales may also be less aware of noise from approaching vessels when engaged in feeding or resting behaviours (Panigada et al. 2006). If whales do spend significant periods of time avoiding oncoming vessels, it could have energetic or survival consequences because foraging and other important activities would be continually disrupted (McKenna et al. 2015).

Between 2004 and 2011, 1 fin whale and 20 humpback whales were reported struck by vessels in British Columbia, Canada (Spaven et al., *unpub*[1]). Four of these strikes were fatal or resulted

[1] Spaven L, Ford J, Cottrell P, Raverty S, Abernethy R, Stredulinsky E. Unpublished report. Occurrences of vessel strikes in Pacific Canadian waters from 2004-2011. Fisheries and Oceans Canada.

in severe, life-threatening injuries (Spaven et al., *unpub*[1]). Humpback whales were the most commonly reported species involved in vessel collisions, with an individual reported injured or killed approximately every 9 months in BC. They were also the most frequently observed species bearing healed or partially healed wounds characteristic of vessel collision injuries (Spaven et al., *unpub*[1]). However, these data were obtained from reports of witnessed vessel strikes and necropsies of recovered carcasses, and thus tend to be biased toward strikes occurring in near-shore areas and involve smaller vessels (rather than larger, ocean-going cargo ships or tankers). For this reason, strike rates for species typically found offshore, such as blue whales and fin whales (Ford et al. 2010, Ford 2014), are probably underestimated in this dataset. Fin whales photo-identified in BC very seldom bear scars attributable to ship strikes (Fisheries and Oceans Canada, Cetacean Research Program, *unpub. data*), which may indicate that most individuals that are hit do not survive being struck (or that few fin whale strikes involve smaller vessels, which are more likely to cause non-fatal wounds) (Panigada et al. 2006).

Due to the difficulty of recovering carcasses for necropsy and obtaining eye-witness reports, documented strike rates may severly underestimate the true impact of vessel collisions on whale populations (Ford et al. 2010, Conn & Silber 2013, McKenna et al. 2015, Spaven et al., *unpub*[1]). Strikes by very large ships often go undetected by ship operators because a collision impact is less likely to be felt and the bows of large ships are not visible to the crew (Conn & Silber 2013, Spaven et al., *unpub*[1]). In fact, many strikes remain unnoticed until arrival at port, when whale carcasses are discovered draped over the bulbous bows of ships (Panigada et al. 2006, Spaven et al., *unpub*[1]). Evidence of ship strikes occurring offshore of the continental shelf break may be particularly difficult to obtain, as carcasses do not refloat in deep water (>1000 m), where hydrostatic pressure prevents the accumulation decomposition gases (Allison et al. 1991, Spaven et al., *unpub*[1]). Ship-struck carcasses from offshore incidents are thus unlikely to strand where they might be properly examined, or pathological evidence to confirm a strike is obscured by decomposition by the time they do eventually wash ashore. Lethal strikes of species with primarily offshore distributions, such as fin whales (Ford et al. 2010, Ford 2014), are probably especially prone to under-reporting for these reasons and pin-pointing the locations of such vessel strikes is extremely difficult without witness reports. To augment the information gathered from necropsies and witnessed reports of vessel strikes, spatial models combining whale distributions and shipping data provide a means of predicting ship strike risk over large areas and identifying the regions of highest conservation concern.

To detect areas of greatest risk and develop meaningful strategies to mitigate ship strikes, the spatial overlap between both affected whale populations and shipping traffic must first be determined. Spatial assessment of variation in average vessel speeds is also critical to identifying areas where strikes are most likely to be lethal. Although the majority (37.5%, N=12) of recently documented collisions (2004-2011) between ships and whales in BC waters occurred off the west coast of Vancouver Island (Spaven et al. in prep.), the risk of vessel strikes in this region has not been assessed. Information about ship strike risk in the offshore areas west of Vancouver Island is particularly vital, given the under-reporting of incidents in these locations (for the reasons discussed above). This is a high-use region for marine traffic, particularly for large commercial ships transiting Juan de Fuca Strait, a major shipping channel that provides access to several large ports (Vancouver, Seattle, and Tacoma). Between 10,000-11,000 vessels of all types enter this confined waterway every year (Nuka Research & Planning Group, LLC 2013). Here, we perform the first spatially explicit analysis estimating the relative risk of lethal collisions between ships and whales off the west coast of Vancouver Island, BC. Our analysis addressed strike risk for the two most frequently observed species of large baleen whales in BC, humpback whales and fin whales. We used systematic aerial survey data (2012-2015) to predict whale densities across the study region, and overlaid these with an AIS marine traffic dataset (2013) to calculate the relative risk of both vessel strikes and collision lethality.

Further, we assess the effect of future maritime traffic projections on relative ship strike risk to investigate the minimum likely increase in risk as a result of projected increases in ship traffic as a result of port expansions and other developments.

MATERIALS AND METHODS

WHALE SIGHTINGS DATA

Cetacean surveys were conducted from a De Havilland DHC-8-102 Dash-8 aircraft that flew along systematically placed transect lines at a nominal speed of 278 km h^{-1} (150 knots) and an altitude of 305 m (1000 ft). Transects ran in a northeast to southwest direction, roughly perpendicular to the west coast of Vancouver Island, BC, Canada at intervals of approximately 16 km. The study area extended approximately 190km from the coast of southwest Vancouver Island and also included the western portion of Juan de Fuca Strait. Two observers were positioned at large observation windows aft of the cockpit (left and right) and reported all whale sightings to a data recorder, who entered them into a laptop computer. Sightings were reported as the whale(s) passed perpendicular to the aircraft; observers measured an angle of declination to each sighting using a clinometer, such that 0° represented a sighting on the horizon, and 90° represented a sighting directly below the airplane. Angles between 70-90° were reported infrequently because this section of the water was generally not visible to the observers (who were scanning through flat, not bubble, windows) when the aircraft was flying on the level. Once a sighting was reported, and if observers required additional time to identify the species and determine the number of individuals, the plane was flown in a loop around the whale(s). Once this was accomplished, the aircraft rejoined the survey transect. Observers also reported environmental conditions (sea state, visibility, precipitation, glare) using standardized categories at 5 min intervals throughout each survey, whenever conditions changed, and at the beginning and end of every transect. Geographic positions along the survey route were recorded automatically using the aircraft's GPS, at a sampling rate of either 1 or 0.2 Hz, depending on the survey year.

Effort and sightings data were filtered for quality control purposes based on the recorded environmental conditions and survey status. Only "on effort" (ON) sightings and survey track lines were included and re-sightings were removed to prevent duplication of data. Additionally, any "on effort, closing" (ONC) track lines, such as loops made by the aircraft to assist in species identification or group size counts, were excluded from the final effort data. The effort tracks and associated sightings that occurred during sea states >4 (Beaufort wind force scale) or when visibility was reduced to ≤5 nm from the aircraft were also excluded. Occasionally, if observers could not positively identify a whale to the species level, but deemed it highly likely to be a particular species based on its morphology or behaviour, it was categorized as 'like humpback whale', 'like fin whale', or 'like grey whale'. Being somewhat common (12% of humpback sightings and 27% of fin whale sightings), these probable sightings were also included in the final sightings tallies used to model whale densities.

To estimate the geographic position of each whale sighting, we used the following procedure. First, we calculated the perpendicular distance of each sighting from the aircraft using a formula from Buckland et al. (2001):

$$d = \frac{a}{\tan\theta}$$

where *d* is the distance (m) of the whale(s) from the transect, *a* is the altitude (m) of the aircraft, and θ is the declination angle (rad) formed between the horizon and the whale(s). We removed sightings without reported angles of declination or where $\theta = 0$ rad, because no horizontal distance could be calculated in these cases. We then calculated the compass bearing to each sighting by adding or subtracting 1.57 rad (90°) from the heading of the airplane (0 rad = north, and heading increases in a clockwise direction) at the time the sighting occurred, depending on whether the sighting was on the right or left side, respectively. Negative bearings and those greater than 6.28 rad (360°) were corrected by adding or subtracting 6.28 rad to obtain the equivalent angle. Using the bearing information, we then estimated the geographic position of each sighting according to the following formulae for determining a destination point by travelling along the shortest distance great circle arc:

$$\psi_2 = \arcsin(\sin\psi_1 * \cos(d/R) + \cos\psi_1 * \sin(d/R) * \cos\theta)$$

$$\lambda_2 = \lambda_1 + arctan2(\sin\theta * \sin(d/R) * \cos\psi_1, \cos(d/R) - \sin\psi_1 * \sin\psi_2)$$

where ψ_1 and λ_1 are the latitude and longitude (rad), respectively, of aircraft at the time the sighting was reported, ψ_2 and λ_2 are the latitude and longitude (rad) of the whale(s), *d* is the horizontal distance (m) from the transect to the whale(s), *R* is the radius of the Earth (6,371,000 m), and θ is the compass bearing (rad) to the whale(s).

AERIAL SURVEY EFFORT

To determine the cumulative area (km^2) that was actually surveyed (and thus account for differences in the spatial distribution of survey effort), we used the following steps to calculate the width of the surveyed area for each transect and then summarized the variation in survey effort across a gridded surface of the study area. We began by constructing an effort buffer on either side of the flown transects to determine the area that was effectively surveyed for whales. We excluded the portion of the transect strip directly beneath the plane, as it was not visible to observers because the survey aircraft had flat windows. Given that observers reported an average maximum sighting angle of θ = 1.22 rad (70º) below the horizon before the downward view became obstructed, and a nominal aircraft altitude of *H* = 305 m, this theoretical blind-spot below the aircraft was calculated according to the following equation (Buckland et al. 2001):

$$2 * H * \tan(90 - \theta)$$

and was found to have a width of 222.6 m (i.e., 111.3 m on either side of the transect line). Our effort buffer thus excluded the strip extending from the transect line to a distance of 110 m on either side of the aircraft. We validated this theoretical blind strip by examining a histogram of the reported sighting distances, and found that sightings became extremely infrequent at distances <110 m from the transect line.

We determined the farthest extent of the effort buffer by constructing a detection function from all ON effort sightings of large baleen whales with the R package ‘Distance’ (Miller 2016 and calculated the resulting effective strip (half-) width (esw) (Buckland et al. 2001). We fit the preliminary detection function using Conventional Distance Sampling (CDS) methods (Buckland et al. 2001, Thomas et al. 2002), with perpendicular distance as the only covariate. Prior to fitting the CDS detection function, four distance outliers (horizontal detection distances >6000 m from the transect) were identified using Cleveland dot plots (Zuur et al. 2010) and removed from the dataset. Candidate detection functions included the hazard-rate and half-normal models, which were evaluated using Akaike’s Information Criterion (AIC). Simple polynomial and cosine expansion terms were also considered. Left truncation was set at 1.25% in the initial detection function to ensure that all sightings <110 m from the transect were excluded (i.e., those inside the blind-spot directly beneath the aircraft). We used Multiple Covariate Distance Sampling (MCDS) after fitting the initial function with CDS to test for possible effects of other covariates. Since these additional covariates were either not significant (i.e., did not improve the model fit – ‘cluster size’, ‘sea state’, and ‘visibility’ covariates) or could not be included due to sample size limitations (‘observer ID’ covariate), we selected the CDS model with the lowest AIC value as the best-fit detection function. The right-truncation distance (*w*) was equivalent to the distance at which detection probability dropped below ~0.10, as recommended by Buckland et al. (2001). All sightings made at distances greater than the truncation distance (*w*) were discounted from further analysis. We estimated goodness-of-fit for the detection function by examining quantile-quantile plots and performing Chi-square and Kolmogorov-Smirnov tests.

We calculated effective strip (half-) width (esw, or μ) according to the following formula (Thomas et al. 2002):

$$\mu = P_a * w$$

where P_a is the probability that a randomly chosen animal within the surveyed area is detected, and *w* is the right-hand truncation distance of the detection function. We constructed the effort buffer such that its farthest extent was equivalent to the effective strip width (μ), since as many whales are detected beyond this distance as are missed within it (Thomas et al. 2002).

In ArcGIS (ESRI 2013) using GME (Geospatial Modelling Environment) (Beyer 2012), we built an effort buffer that extended from the left truncation distance (110 m) to the esw (1010 m) on either side of the surveyed transects. We then divided our survey area into a grid of 25 km^2 cells and calculated the aggregate area surveyed per cell by summing the total area of overlapping effort buffers contained within each cell. Only cells that contained survey effort (i.e., buffer area > 0 km^2) were retained for subsequent analysis (N=1636). The whale sightings, corrected for geographic position and weighted by cluster (group) size, were then summed within each of these grid cells.

VESSEL TRAFFIC DATA

We analysed the spatial distribution of marine traffic throughout the study area using an Automatic Identification System (AIS) data set collected by the Canadian Coast Guard (CCG) in 2013. AIS-equipped vessels broadcast information about their position, course, and speed over ground (SOG) using VHF radio signals, at sampling rates of several times per minute. Simard et al. (2014) compiled these AIS data and binned the resulting traffic densities (measured in daily ship-h, averaged over the entire year) into five categories of ship speed (Table 1) across a grid of 1 km^2 cells. Ship speeds were determined from AIS positions using a multi-step filter that excluded speeds >40 knots and smoothed sudden changes in speed using a 900 s moving average (Simard et al. 2014). Vessels not underway and stationary AIS fishing beacons (i.e., SOG ≤1 knot) were removed from the data set. Additionally, our analysis excluded the slowest traffic category (2-5 knots) reported by Simard et al. (2014), as vessels travelling at such low speeds are unlikely to pose a lethal strike risk to whales (Vanderlaan & Taggart 2007). The 2013 AIS dataset consisted of all compulsory AIS-reporting traffic (ships other than fishing vessels ≥500 gross tons (GT), ships ≥300 GT transiting international boundaries, and ships ≥150 GT travelling internationally and carrying >12 passengers), as well as vessels voluntarily equipped with AIS. Marine traffic included in the 2013 AIS data set can be generally categorized into the following types: cargo (e.g., container ships, bulk carriers), tanker, passenger (e.g., cruise ships, ferries), tug and towing, fishing, and pleasure vessels (Simard et al. 2014). The first three categories (cargo, tanker, and passenger) are likely of most concern when assessing lethal ship strike risk to whales, given the typically greater size and speed of these vessel types. More detailed information about AIS data collection and processing is provided by Simard et al. (2014).

RELATIVE PROBABILITY OF A WHALE-VESSEL ENCOUNTER

Modeling the predicted densities of humpback and fin whales

Determining the relative probability of a ship strike (using the proxy of a whale and a vessel occupying the same grid cell) requires estimates of the relative probability of encountering whales and the relative probability of encountering vessels across all grid cells (Vanderlaan et al. 2008). To accomplish this, we first estimated the predicted densities of humpback and fin whales (individuals/25 km^2 cell) from the aerial survey sightings using generalized additive models (GAMs). Modelling of whale densities was limited to these two species, as other baleen whale species were either not observed during the aerial surveys (e.g., North Pacific right whales, sei whales) or were sighted so infrequently that construction of a spatial model was not possible (e.g., blue whales, grey whales and minke whales; Table 2). Prior to model construction, we undertook data exploration following the protocol described by Zuur et al. (2010) to ensure that underlying model assumptions were not violated. One outlier was removed from the humpback count data because this grid cell contained a single sighting but had a very small surveyed area (0.03 km^2), resulting in a misleadingly low predicted density that substantially influenced the dispersion of the data set. Potentially nonlinear relationships between explanatory variables and whale counts were assessed prior to inclusion in the candidate GAMs by building separate generalized linear models (GLMs) and fitting GAMs to the GLM residuals for each covariate in turn. Variables that displayed non-linear relationships with the GLM residuals and effective degrees of freedom (edf) > 1 were included as smoothers in the final negative binomial GAMs, whereas those with edf = 1 were included as beta terms. We constructed a set of candidate GAMs with latitude (converted to UTM), slope and depth as possible explanatory environmental variables (Table 3). Longitude was excluded as an explanatory variable, as it was highly correlated with depth (r=0.76, p<0.0001) in our study area. An offset term to account for the relative survey effort per cell (aggregate buffer area in km^2) was also included in all of the candidate models.

We fit negative binomial GAMs (logarithmic link function) in R using the ‘mgcv’ package (Wood 2004, 2011) at a spatial resolution of 25 km^2 for both species, and then used these models of whale distribution to predict humpback and fin whale densities across the study area at a resolution of 1 km^2, to match the AIS ship data. The larger (25 km^2) scale was chosen as the grid resolution at which to fit the GAMs because this scale was deemed more biologically relevant for predicting the distribution of whales. Changes in the environmental covariates (UTM northing, slope, and depth) at a 1 km^2 resolution are likely too fine-scale to noticeably influence the distribution of large cetaceans. During model fitting, the appropriate smoothness for each covariate term was estimated using likelihood-based methods (REML). The negative binomial error distribution was chosen for fitting the GAMs, as the response variable (N) consisted of over-dispersed (zero-inflated) count data, and global GAMs took the general form:

$$N \sim s(UTM\ northing) + \ s\left(\sqrt{|depth|}\right) + \mathrm{slope} + offset(\ln(effort))$$

The depth covariate was square root transformed to make this predictor variable more uniform and thus reduce differences in the leverages of individual data points, which helps to stabilize model predictions (Wood 2006). We selected the best-fit GAMs for predicting densities of humpback whales and fin whales by comparing the AIC scores (Zuur et al. 2009) of the various candidate models generated from this global model. Candidate models were chosen by using backwards selection to drop non-significant covariates from the global model. GAM over-fitting was avoided by incorporating the multiplier gamma=1.4 (Kim & Gu 2004) to inflate the effective degrees of freedom (edf) in the REML score. To assess whether or not spatial autocorrelation was present in the model residuals, we plotted variograms using the ‘gstat’ package in R

(Pebesma 2004), and also examined the distribution of residuals by size over the *x-y* coordinates of the study area.

Estimating probability of encountering whales and vessels

We used the GAM-predicted whale densities from the top-ranked models to estimate the probability of observing a humpback or fin whale ($P_{rel}(Whale)_i$) within each grid cell (*i*), relative to all other grid cells (*n*), with an approach adapted from Vanderlaan *et al.* (2008):

$$P_{rel}(Whale)_i = \frac{W_i}{\sum_{i=1}^{n} W_i}$$

where W_i was the predicted density of whales within each cell (individuals/km^2), as estimated by each negative binomial GAM. We calculated $P_{rel}(Whale)_i$ separately for fin whales and humpback whales.

We likewise standardised the vessel traffic intensity values to determine the relative probability of observing a ship ($P_{rel}(Vessel)_i$) within each grid cell *i,* over the total study area of *n* cells (Vanderlaan et al. 2008):

$$P_{rel}(Vessel)_i = \frac{V_i}{\sum_{i=1}^{n} V_i}$$

where V_i was the annual average of daily ship-hr/km^2 (vessels travelling at speeds ≥5 knots) within each cell, *i*.

The relative probability that a whale and a vessel encounter one another (i.e., occupy the same cell), was used as a proxy for the risk of a vessel striking a whale within each grid cell, *i,* in a domain of *n* cells (Vanderlaan et al. 2008):

$$P_{rel}(Encounter)_i = \frac{P_{rel}(Whale)_i \times P_{rel}(Vessel)_i}{\sum_{i=1}^{n}(P_{rel}(Whale)_i \times P_{rel}(Vessel)_i)}$$

where estimates of $P_{rel}(Encounter)_i$ were also standardised such that their sum in the domain of *n* grid cells was equal to 1. $P_{rel}(Encounter)_i$ was calculated for fin whales and humpback whales separately.

RISK OF A LETHAL STRIKE BASED ON SHIP SPEED

We determined the mean vessel speed (knots) per surveyed grid cell ($Speed_i$) using the following formula:

$$\bar{X}_i = \frac{\sum_{c=1}^{n}(\bar{X}_c \times Density_c)}{\sum_{c=1}^{n} Density_c}$$

where $\bar{X}_c$ was the median speed of each vessel speed class (Table 1; *N*=4, 2013 AIS), and $Density_c$ was the vessel traffic intensity (mean annual daily ship-hr) per cell (*i*) for each speed class (*c*) . We then determined the probability that a ship strike would inflict a lethal injury using the mean vessel speed per cell ($\bar{X}_i$) and the simple logistic regression model (Conn & Silber 2013; Figure 1):

$$P(Lethal)_i = \frac{1}{1 + exp^{-(-1.91+0.22\bar{X}_i)}}$$

We then estimated the relative risk of a lethal collision between a vessel and a whale as follows (Vanderlaan & Taggart 2007):

$$RR_{\boldsymbol{i}} = P_{\boldsymbol{rel}}(Encounter)_i \times P(Lethal)_i$$

To identify areas with the highest relative risk of collisions and mortality due to collisions, we extracted the grid cells representing the 95th percentile of $P_{rel}(Encounter)_i$ and RR_i values for both humpback and fin whales, and compared these regions to the remainder of the study area. Probabilities of whale, vessel, and whale-vessel encounters (i.e., ship strikes), as well as mean ship speed and relative risk of lethal whale-vessel encounters, were mapped for humpback and fin whales using the 'PBSmapping' package (Schnute et al. 2015) in R. All summary statistics are presented as mean ± standard deviation, unless otherwise specified.

PROJECTED INCREASE IN MARINE TRAFFIC & FUTURE SHIP STRIKE RISK

To quantify the potential impact that future growth of the marine shipping industry could have on ship strike risk in the study area, we obtained current and future estimates of shipping activity from a quantitative risk assessment report prepared for the proposed Roberts Bank Terminal 2 (Herbert Engineering Corp. and Environmental Research Consulting 2014) and applied these to the ship strike risk models. These shipping data included an estimate of the number of ships (by ship type; Table 6) travelling into and out of Juan de Fuca Strait and the southern Strait of Georgia in 2012, as well as predicted numbers of ships in 2030. Since the Herbert Engineering Corp. and Environmental Research Consulting (2014) projections of future marine traffic did not include all Puget Sound destined ships, we also considered a second data source prepared by the Friends of the San Juan Islands and San Juan Islanders for Safer Shipping (2015). The baseline (i.e., current) shipping transits from this report (~2015) appear to include the same Canadian port sources as the Herbert Engineering Corp. and Environmental Research Consulting (2014) report, although it does not include cruise ships. The future projections (not attributed to a specific year) appear to include the sources reported in the Herbert Engineering Corp. and Environmental Research Consulting (2014) report, as well as additional proposed expansions in U.S. waters (Table 7). We excluded vessel transits associated with activities that were primarily restricted to the Strait of Georgia from our analysis, as these transits do not occur in our study area. For the purposes of modelling the future projected traffic, we assume that the 2012 (Table 6) and 2015 (Table 7) shipping data account for most of the ship traffic of concern captured in the Simard et al. (2014) AIS data set (i.e., large, ocean-going vessels travelling at speeds ≥10 knots), and thus, these data are reasonably representative of the traffic data used in our previous analyses. Furthermore, we assume that there is no difference in the ship population from 2012 to 2015, and thus the traffic behaviour of this ship population is represented by the 2013 AIS traffic data.

To determine how ship strike risk to humpback and fin whales might change with these anticipated increases in maritime traffic on the southern BC coast, we compared our existing analysis of current strike risk (based on the 2013 AIS ship data) to strike risk analyses that incorporated proportional changes in ship traffic expected in the future (based on the ship data presented in the two reports described above). Since the shipping projections reports both classified vessels by type, rather than by speed, we first categorized ship types into speed classes according to the mean speed at which they are expected to travel. Most large ocean-going vessels (container ships, bulk carriers, chemical carriers, and cargo ships) travel at mean speeds of 10-15 knots, while tankers and cruise ships travel slightly faster at 15-20 knots (Simard et al. 2014). We applied the proportional changes in future traffic (Tables 6 & 7) as multipliers to the shipping intensity per cell (mean daily ship-hr/km^2) for these two speed categories (10-15 and 15-20 knots) from the 2013 AIS data. However, we only applied the multipliers to those cells with mean daily ship-hr values >0.0025 (top 5 of 6 traffic density classes, defined by Simard et al. 2014), to approximate the most likely routes taken by the future traffic – all of which are large commercial ships. We then repeated our analysis (in the same manner as described above for the 2013 AIS ship traffic data) to obtain the relative risk of lethal strikes to humpback and fin whales that is anticipated in the future. For clarity, we refer to the proportional changes in future ship traffic as the ‘Herbert’ and ‘San Juan’ multipliers throughout the remainder of this report.

RESULTS

WHALE SIGHTINGS DATA & AERIAL SURVEY EFFORT

We conducted aerial surveys on 34 days from 2012-2015, during all months of the year except April, May and August (Figure 2). The majority of surveys took place in the fall and winter months, with the greatest number occurring in September (N = 11; Figure 2). All survey effort and sightings were aggregated and analysed as a single data set, as there were insufficient data to examine annual or seasonal trends in whale spatial distribution. Excluding those sections with poor environmental conditions, or where the plane flew in a closing loop, or that were flown at altitudes >366m, we surveyed a total of 21,801 km of “on effort” line transects.

The detection function with the lowest AIC value (4054.86) was a CDS hazard rate model with no expansion terms and a right truncation distance (w) of 2650 m (Figure 3). From this detection function, we calculated the effective strip (half-)width (esw, µ), or the farthest extent of the effort buffer, as 1010 m on either side of the aircraft. The aggregated effort buffers from all 34 surveys comprised a total surveyed area of 39,120 km^2. After filtering for weather conditions, effort status, and altitude, 276 of the 322 total sightings (Table 2) with distances less than the truncation distance (2650 m) remained. This included a total of 159 humpback whale or ‘like humpback whale’ sightings (329 individuals), and 74 fin whale or ‘like fin whale’ sightings (120 individuals; Figure 4), which were input into the GAMs following the exclusion of a single outlier in the humpback sighting data. Mean group size per sighting for humpback whales was 2.1 ± 3.5 individuals (range = 1-33), and mean group size for fin whales was 1.6 ± 1.0 individuals (range = 1-5; Figure 4). There were also three sightings of single blue whales (Table 2), all of which were observed west of the continental shelf break (200 m isobath; Figure 4).

VESSEL TRAFFIC DATA

The 2013 AIS vessel data indicated that shipping traffic was less dense offshore, but became much more concentrated as it funnelled into or out of Juan de Fuca Strait (Figure 5a). In particular, a commonly-transited route is apparent that begins offshore (around latitude 48.5° N and longitude 128.0° W) and becomes more heavily used by ships as it moves eastward, toward the entrance of Juan de Fuca Strait and its Traffic Separation Scheme (TSS) lanes. Mean shipping intensity per grid cell for the entire study area was 0.006 ± 0.018 daily ship-hr/km^2 (range = 0.44 daily ship-hr/km^2) and the mean relative probability of encountering a vessel per cell, $P_{rel}(Vessel)_i$, was $4.2 \times 10^{-5} \pm 12.3 \times 10^{-5}$ (range = 0-0.003). AIS-reporting traffic in 2013 (excluding the slowest 2-5 knot speed category and cells without traffic) travelled at mean speeds per cell exceeding 12 knots throughout most of the study area ($\overline{X}_i$ = 12.5 ± 1.8 knots, range = 7.5-21.4 knots; Figure 5b). Vessel speeds were the highest (≥16 knots) near the continental shelf break (200 m bathymetric contour) at the northern end of the study area, offshore of the shelf break, and inside Juan de Fuca Strait (Figure 5b). Regions with average vessel speeds ≤10 knots were limited, and primarily occurred closer to the Vancouver Island shore and at one location along the southern portion of the continental shelf break (Figure 5b). Slow speeds at this location on the shelf break are likely the result of the contribution of speeds from vessels engaged in fishing activities in that area (see Figure 13 in Simard et al. 2014).

RELATIVE PROBABILITY OF A WHALE-VESSEL ENCOUNTER

The top-ranked GAM for predicting humpback whale densities included both latitude (UTM northing) and depth as explanatory variables, while the top-ranked GAM for fin whale densities only included depth (Table 3). Model averaging was not applied to the two highest ranked fin-whale GAMs (despite ΔAIC < 2; Table 3); we retained the simpler model with only the depth smoother because the latitude term was non-significant in the global model (p-value = 0.22). Model fits were significantly improved when depth was square-root transformed (versus identical models using untransformed depth data). A 2-dimensional smoother term incorporating depth and latitude was not considered in the candidate models because non-additive interactions between these variables were not detected. Detailed summaries of GAM outputs are presented in Tables 4 & 5. The top-ranked GAMs predicted mean densities of 0.008 ± 0.014 individuals/km^2 (max = 0.089) for humpback whales and 0.003 ± 0.002 individuals/km^2 (max = 0.005) for fin whales. Smooth terms selected in the top-ranked models indicated that relationships between the significant environmental covariates and whale density were non-linear (Figure 6). The model smoothers for humpback whales predicted higher densities of individuals at the lowest latitudes in the study area (~48.1°, or level with Cape Flattery and the Washington state coast) and at intermediate latitudes (~49.3°, or level with Nootka Island and Hesquiat Peninsula on the Vancouver Island coast) (Figure 6). The highest densities of humpback whales were predicted to occur at depths of ~200 m (Figure 6), which represents the edge of the continental shelf in our study area (the continental slope begins around the 200 m bathymetric contour and eventually levels out again starting at the 2300 m contour, where it reaches the abyssal plain). The highest densities of fin whales were predicted by the smoothing term to occur off the edge of the continental shelf, in water depths exceeding 450 m (Figure 6). Regions with the highest relative probabilities of encountering whales (per 1 km^2 cell) reflected the predictions of the GAM smoothers: humpbacks were most likely to be found along the continental shelf edge (200 m isobath) and in the western portion of Juan de Fuca Strait (Figure 7a), while fin whales were most likely to be found offshore of the shelf break (>450 m; Figure 7b). Fin whale encounter probability was very low inshore of the shelf break (Figure 7b). Predictive power of the top-ranked humpback density model was fairly high, with 66.1% deviance explained, while the top-ranked fin whale model had a lower explained deviance of 26.7%. This lower explained deviance is likely due to the fact that only a single explanatory covariate (depth) was retained as significant in the top-ranked model.

The mean relative probability of a vessel encountering a whale (i.e., relative risk of a ship strike) off the west coast of Vancouver Island was $4.2 \times 10^{-5} \pm 23.8 \times 10^{-5}$/km^2 (max = 0.007/km^2) for humpback whales and $4.2 \times 10^{-5} \pm 6.3 \times 10^{-5}$/km^2 (max = 0.001/km^2) for fin whales. Humpback whales were most likely to be struck along the continental shelf break, the inshore approaches to Juan de Fuca Strait (east of 200 m isobath, ~48.5° N), and within the western portion of the strait itself (Figure 7c). The mean collision probability with humpback whales was 32.3-fold higher in these areas (95th percentile) compared to the rest of the study domain. Fin whales were most likely to be struck in the offshore approaches to Juan de Fuca Strait (west of the 200 m isobath, ~48.5° N) and inside the western portion of the strait (Figure 7d), where collision probability was 7.7-fold higher than the rest of the study domain.

RISK OF A LETHAL STRIKE BASED ON SHIP SPEED

Across the whole study area, the mean relative risk of lethal ship strikes was $0.3 \times 10^{-4} \pm 1.8 \times 10^{-4}$/km^2 for humpback whales (Figure 6e) and $0.3 \times 10^{-4} \pm 0.5 \times 10^{-4}$/km^2 for fin whales (Figure 6f). In regions with the greatest risk of lethal ship strikes (95th percentile; Figure 8), we estimated the mean relative risk of lethal collisions with humpback whales to be $3.7 \times 10^{-4} \pm 6.9 \times 10^{-4}$/km^2, a 35.2-fold increase compared to the remainder of the study area. These regions of highest relative lethal strike risk for humpbacks included Juan de Fuca Strait, an area due west of its entrance and inshore of the continental shelf break, and some areas overlying the 200 m bathymetric contour along the shelf break itself (Figure 8). For fin whales, the regions of highest concern had a mean relative lethal strike risk of $1.8 \times 10^{-4} \pm 1.1 \times 10^{-4}$/km^2 (Figure 8), an 8.1-fold increase over the rest of the study area. Areas with the highest relative risk of lethal collisions with fin whales included Juan de Fuca Strait, as well as an area due west of its entrance (48.5° N) but offshore of the continental shelf break (Figure 8). Within the areas of highest lethal strike risk (Figure 8), we estimated a mean value of $P(Lethal)_i$ of 0.70 ± 0.09 for humpback whales and 0.75 ± 0.04 for fin whales, compared to a mean of 0.68 ± 0.10 (both species) in the remainder of the study area. In other words, a whale that is struck in these high risk areas has a 70% (humpbacks) or 75% (fin whales) chance, on average, of being killed, compared to a 68% chance elsewhere in the study domain.

PROJECTED INCREASE IN MARINE TRAFFIC & FUTURE SHIP STRIKE RISK

With the proportional changes in maritime traffic predicted in the Herbert Engineering Corp. and Environmental Research Consulting (2014) assessment (2014), the mean intensity of shipping in the most frequently transited portions of our study area (i.e., cells >0.0025 daily ship-hr) is expected to increase from 0.011 ± 0.024 to 0.014 ± 0.034 daily ship-hr/km^2 by 2030. For humpback whales, the mean future relative risk of lethal strikes in the highest risk locations (95th percentile, see Figure 8), as predicted by the Herbert multipliers, was ~1.1 times greater, increasing from $3.7 \times 10^{-4} \pm 6.9 \times 10^{-4}$/km^2 in 2013 to $4.2 \times 10^{-4} \pm 8.0 \times 10^{-4}$/km^2 in 2030. This means that in 2030, a 44-fold difference in the average risk of lethal strikes to humpbacks is predicted within the highest risk locations as compared to the rest of the study area (up from the 35.2-fold difference estimated in 2013). For fin whales, the Herbert multipliers predicted that the mean relative risk of lethal strikes in areas of greatest concern (95th percentile) would increase by ~1.2 times, up from $1.8 \times 10^{-4} \pm 1.1 \times 10^{-4}$/km^2 in 2013 to $2.2 \times 10^{-4} \pm 1.5 \times 10^{-4}$/km^2 in 2030. This represents an 10.5-fold difference in average lethal strike risk between high-risk locations and the remainder of the study area in 2030, as compared to the 8.1-fold difference estimated in 2013. The predicted mean lethality within high-risk areas also increased from 2013 to 2030 for both humpbacks (0.75, up from 0.70) and fin whales (0.77, up from 0.75). This means that in 2030, whales would have a greater than 75% chance of being killed if they are struck by vessels in these locations.

The San Juan multipliers predicted an even greater future increase (~3-fold) in mean shipping intensity along the most transited routes (cells >0.0025 daily ship-hr): from a mean of 0.011 ± 0.024 daily ship-hr/km^2 in 2013 to 0.030 ± 0.096 daily ship-hr/km^2 in the future. Within the areas of highest relative risk (95th percentile), the mean estimated risk of lethal collisions with humpback whales increased by ~1.5 times, from $3.7 \times 10^{-4} \pm 6.9 \times 10^{-4}$/km^2 in 2013 to $5.6 \times 10^{-4} \pm 10.4 \times 10^{-4}$/km^2 after planned terminal and refinery expansions. Relative risk of lethal collisions with fin whales in areas of greatest concern increased by ~2.2 times, from $1.8 \times 10^{-4} \pm 1.1 \times 10^{-4}$/km^2 in 2013 to $3.9 \times 10^{-4} \pm 2.9 \times 10^{-4}$/km^2 in the future. These future increases represent a 95.0 and 27.4-fold difference (humpbacks and fin whales, respectively) in the mean relative risk of lethal ship strikes between the areas of highest concern and the remainder of the study area (up from the 35.2 and 8.1-fold differences estimated in 2013). In the future, predicted mean lethality within high-risk areas also increased for both humpbacks (0.84, up from 0.70 in 2013) and fin whales (0.83, up from 0.75 in 2013). This means that after the planned expansion of maritime traffic anticipated in the San Juan Islanders shipping report, whales that are struck by vessels in these high-risk locations would almost certainly be killed (~84% chance of mortality).

DISCUSSION

GAMs proved to be an effective and powerful method for estimating continuous, quantitative gradients of whale density across our study area using discrete point observations of individual whales. Spatial distributions of whale encounter probabilities (Figure 7a, b) estimated from these GAM-predicted densities corroborate existing information about humpback and fin whale distributions in British Columbia. We determined that humpback whale distribution off south-western Vancouver Island could be predicted based on latitude (UTM northing) and water depth, a conclusion that is supported by similar models (Williams & O'Hara 2009, Dalla Rosa et al. 2012) applied to humpback sightings over larger areas of the B.C. coast. Dalla Rosa et al. (2012) determined that humpbacks primarily favoured mid-shelf waters (50-200 m), which matches our finding that humpback densities increased around the continental shelf break (Figure 7a). Ford (2014) likewise describes humpback feeding areas in BC as primarily occurring in coastal or shelf waters, and models based on whaling catch locations also indicate that humpbacks were predominately distributed inshore of the shelf break (Gregr & Trites 2001). Although Dalla Rosa et al. (2012) predicted maximum humpback densities at slightly shallower depths (100 m) than our model (200 m; Figure 6), this is likely due to their larger study area that covered the entire BC coast. The shelf break in our smaller study domain off Vancouver Island occurs much farther from shore than in the rest of BC and the slope between the 100-200 m isobaths is also more gradual. This means that the 100 m isobath is not located near the shelf break off Vancouver Island, as it is in other coastal regions (e.g., Haida Gwaii), and thus maximum humpback densities in our study area can reasonably be expected to occur in somewhat deeper water. In California, Dransfield et al. (2014) similarly predicted that humpbacks had an affinity for the shelf break and occurred at greatest frequencies near the 200 m isobath. Like our model, Dalla Rosa et al. (2012) found that latitude was a significant predictor of humpback densities, and suggested this might occur because the extent of preferred, on-shelf habitat varies greatly by latitude in BC. Off Vancouver Island, the continental shelf ranges between 5 and 75 km wide, depending on latitude (Barrie et al. 2014). Higher humpback whale encounter rates are expected in regions where the continental shelf is wider, as more of the primary productivity is retained on-shelf in these areas, thus remaining available to coastal food webs (Perry et al. 1989, Ware & Thomson 2005). However, while the highest humpback densities in our study area were predicted at the lowest latitudes (~48°N) where the area of shelf habitat is also greatest, there was also an increase in estimated humpback density that occurred further north (~48.5°N), where the shelf is actually narrower. It is likely that gradients in large whale densities with respect to latitude and/or depth are predominantly caused by underlying differences in prey availability in relation to these habitat variables (Dalla Rosa et al. 2012).

Our fin whale distribution model also matched that of Williams & O’Hara (2009) in that depth was a significant predictor of density, however, we did not find that fin whales were associated with latitude features. This difference is most likely due to the smaller size of our study area, which comprised a much narrower latitudinal range than Williams & O’Hara (2009). Past fin whale sightings in BC have been primarily located in deep water beyond the continental shelf break (Ford 2014), which supports our model’s predictions (Figure 7b). Habitat models based on whaling catch records for fin whales in BC also confirm that this species’ distribution is largely offshore of the continental shelf (Gregr & Trites 2001). Although fin whales also regularly occur in certain inshore areas (Gregr & Trites 2001, Ford 2014), none of these coastal habitats are located within our study domain. While quantitative information about the specific distribution of fin whales by depth is not available for BC, fin whale distribution studies in the Mediterranean Sea also indicated that this species is primarily found in offshore waters beyond the continental shelf (Forcada et al. 1996, Panigada et al. 2008). As in our model (Figure 6), the highest densities of fin whales in the Mediterranean occurred at depths exceeding 1000 m, and declined sharply with decreasing depth (Panigada et al. 2008).

GAM-predicted mean densities of humpback whales (0.008 individuals/km^2) were more than double that of fin whales (0.003 individuals/km^2). This is consistent with recent assessments and surveys of cetacean abundance in BC, which report humpbacks as the most commonly observed species of baleen whale (Ford et al. 2010, Dalla Rosa et al. 2012, Ford 2014). These higher densities reflect the strong population recovery that humpbacks have undergone since the end of commercial whaling in BC. Fin whales, although increasing in number, remain designated as 'Threatened' (Fisheries and Oceans Canada 2013a, Ford 2014). The smaller relative population size of fin whales is reflected in the lower densities of this species (and probability of encounter) predicted by our model (Figure 7), as well as the lower frequency (and mean group size) of fin whale sightings during the aerial surveys (Figure 4). We found only a small degree of overlap between model-predicted humpback and fin whale distributions (Figure 7a, b), suggesting the possibility of habitat partitioning in regard to prey type and/or patch characteristics (Zerbini et al. 2006). Such partitioning is possible, since fin whales primarily consume euphausiid zooplankton, whereas humpback diet is more diverse and includes both zooplankton and small schooling fish (Flinn et al. 2002, Ford 2014).

The mean densities of humpback whales (0.008/km^2) and fin whales (0.003/km^2) predicted by our GAMs are also biologically reasonable, in that they are comparable to density estimates from studies of the same species in other regions of the Pacific and worldwide. For instance, Zerbini et al. (2006) estimated densities of 0.012 humpbacks/km^2 and 0.007 fin whales/km^2 off the Alaskan Peninsula and Aleutian Islands. Campbell et al. (2015) predicted somewhat lower mean densities of 0.003 humpbacks/km^2 and 0.001 fin whales/km^2 off the coast of southern California (all years and seasons combined). In the Atlantic, Bezamat et al. (2014) reported humpback whale densities of 0.008-0.018 individuals/km^2 during peak breeding season along the coast of Brazil, and in the enclosed seas of the western Mediterranean, fin whale densities have been predicted to be 0.010/km^2 (Gannier 2006) and 0.024/km^2 (Forcada et al. 1996).

It is important to note that our model estimates of humpback and fin whale densities off Vancouver Island are conservative relative to true whale densities, which are likely significantly higher. This means that predictions of relative lethal strike risk calculated from the model-estimated whale densities should also be interpreted as conservative, minimum estimates. We were not able to correct for missed animals resulting from either availability bias (probability that a whale will be at the surface when the plane passes overhead, and thus be available for observers to detect), or from detection bias (probability that a whale will be detected by an observer when it is at the surface) (Buckland et al. 2001). Such corrections would result in higher (and also more accurate) density estimates, but likely would not alter the spatial distribution of the whale density predictions. It is this spatial pattern and the relative differences in density between species (humpback and fin whales), and between various regions in the study area for each species, that provide the most important information from the ship strike risk analysis. In other words, regardless of the numeric density estimates, the spatially explicit predictions of higher risk areas are the important result from a conservation perspective. Another limitation of the models we have employed is that they were composed of only one or two static explanatory variables. While this provides a good indication of the year-round, general distributions of humpbacks and fin whales, future models could improve upon both the spatial and temporal resolution of predicted whale densities by incorporating additional covariates. In particular, dynamic, time-varying environmental predictors might reveal temporal fluctuations in whale distribution throughout the study area that would be important in mitigating ship-whale collisions.

Vessel traffic encounter probabilities in the study area increased toward the entrance of Juan de Fuca Strait (Figure 5a), as this represents an area where ships leave the open sea and traffic becomes concentrated as it enters designated shipping lanes, before proceeding to various ports near Vancouver and Seattle (Herbert Engineering Corp. and Environmental Research Consulting 2014). The reverse occurs for vessels departing Juan de Fuca Strait, with the routes gradually fanning out in different directions, leading to lower ship encounter probabilities farther offshore. The route into and out of the Strait is regularly transited by large, deep sea vessels (Herbert Engineering Corp. and Environmental Research Consulting 2014), and the vast majority of AIS-reporting traffic moving through this area are cargo or tanker type ships (Simard et al. 2014). These vessel types are of particular concern when assessing ship strike risk, as their large size (container ships are often >300 m long with a beam of >40 m; Herbert Engineering Corp. and Environmental Research Consulting 2014) and high speeds (typically 10-20 knots) mean that collisions with whales will most likely be lethal. Vessel speed is positively related to strike lethality: ship speeds exceeding 10 knots are more likely than not to cause mortality (Figure 1), and speeds ≥18 knots are almost certain to be lethal (Vanderlaan & Taggart 2007, Conn & Silber 2013). Higher vessel speeds are correlated with shorter contact durations and increased accelerations experienced by struck whales, both of which lead to increased impact severity, and presumably, greater tissue damage (Silber et al. 2010). Mean vessels speeds were >12 knots throughout the majority of cells in our study area off southwest Vancouver Island (Figure 5b), which, in the event of a vessel strike, corresponds to a lethality probability of ~0.67 (Figure 1). In other words, throughout most of the study domain, whales struck by vessels would have more than a 67% chance of being killed. Higher vessel speeds are not only associated with greater strike mortality rates, but also lead to increased collision frequencies; ships involved in vessel strikes are often travelling at greater than average speeds (Conn & Silber 2013, Lammers et al. 2013, Spaven et al. in prep.). In addition to direct strikes, large ships travelling at high speeds are also more likely to collide with whales as a result of hydrodynamic draw, which can pull a nearby whale toward a vessel's hull (Silber et al. 2010).

We predicted the highest probabilities of whale-ship encounters (strikes) in regions where high whale densities co-occur with high-intensity maritime traffic, namely along the continental shelf break at the 200 m isobath (humpbacks), offshore of the shelf break (fin whales), and inside Juan de Fuca Strait and the area west of its entrance (both species). Regions of highest risk for lethal collisions closely mirrored those with the highest incidence of strikes, since mean vessel speeds exceeded 12 knots throughout most of the study area. Even though fin whales occurred at much lower densities than humpback whales, the mean relative risk of a lethal collision per cell was actually quite similar for these species (0.30×10^{-4} versus $0.29 \times 10^{-4}/\text{km}^2$ for humpbacks). This is likely related to the primarily offshore distribution of fin whales (Figure 7a), which exposes them to marine traffic travelling at higher mean speeds (Figure 5b), and thus results in equally high probabilities of lethal injury in the event of a strike, despite their lower densities.

We did not account for species-specific differences in vulnerability to ship strikes, and for fin whales, this may mean that our risk estimates are low. Worldwide, fin whales are the most frequently struck by vessels (Laist et al. 2001). Fin whale dive behaviour or anatomy may make them more vulnerable to lethal vessel strikes than other species, which our model did not take into account. The larger body size and more streamlined body shape of fin whales (Ford 2014) may limit their manoeuvrability and help to explain why they are more vulnerable to lethal strikes than humpback whales. Behavioural and physical factors that increase the vulnerability of some cetacean species to ship strikes include longer surface intervals, larger body size, limited ability to avoid approaching vessels due to either swim speed or manoeuvrability constraints, and auditory limitations such as directionality and distance perception (Lawson & Lesage, *unpub*[2]). From a conservation standpoint, ship strike mortalities may also have a proportionally greater impact on the fin whale population because this species has a lower overall abundance than humpback whales. Estimates of Potential Biological Removal (PBR) give an indication of the threshold above which human-caused mortality affects population recovery. PBR is an estimate of the maximum number of animals (excluding natural mortality) that may be removed per year, while still allowing the population to reach or sustain its 'optimum sustainable population' (Wade 1998). PBR estimated for humpback whales in the Canadian Pacific, based on a population estimate in 2006 of 2145 individuals (range = 1970-2331), was 21 whales/y (Ford et al. 2009). It is unlikely that a PBR estimate for fin whales would allow for more mortality than this, given the overall comparatively lower abundance of this species in BC (Ford 2014).

Despite having very low predicted encounter probabilities for fin whales, and only moderate encounter probabilities for humpbacks (Figures 7a, b), Juan de Fuca Strait is a relatively high risk area for lethal collisions with both species. This is likely due to a combination of factors: the strait has a very high intensity of vessel traffic (Figure 5a) and higher than average vessel speeds (Figure 5b). Therefore, any whales found within Juan de Fuca Strait, however infrequently, are exposed to high risk of a lethal collision. In addition, GAMs always predict non-zero densities of whales across every cell in a study domain, not just those in which actual sightings were recorded – so cells where fin whales are unlikely to occur will actually show positive (albeit very small) density estimates, which translate into high whale-ship encounter probabilities in areas where vessel traffic is very intense. Although no fin whales were observed inside Juan de Fuca Strait during our aerial surveys, infrequent sightings of fin whales have been reported in the Salish Sea (Ford 2014, Chamberlain 2015, Mark Malleson, Prince of Whales Whale Watching, Victoria, BC. November 2015, *pers. comm.*), indicating that fin whales do occasionally enter the Strait. For this reason, we believe the predicted increased strike risk to fin whales within the Strait is reasonable, in the rare instances that they are found in this location. Furthermore, vessel strike probabilities within the Strait could also be even higher than our model predicts, as the traffic lanes result in a confined navigational space in which vessels are limited in their ability to manoeuvre around whales. In other studies, physical bottlenecks where marine traffic becomes concentrated (like Juan de Fuca Strait) have similarly been associated with increased strike risk (Williams & O'Hara 2009, Silber et al. 2010). However, further study and data collection, in the areas of high vessel density in the study area, would be useful to refine our estimates of whale distribution and behaviour.

Our analysis was based on an aggregate data set of all aerial survey sightings (2012-2015) and all vessel traffic (2013), regardless of season. Although vessel encounter probabilities represented an average of year-round traffic in the study area, whale surveys were not conducted in every month of the year, and a large number were conducted in a single month (September, Figure 2). We therefore could not identify seasonal variations in the density and distribution of whales, a factor which is likely to impact ship strike risk. Strike rates would increase at times of year when whales are most abundant in an area, or when marine traffic is highest, if indeed there is a seasonality to commercial shipping (Panigada et al. 2006, Lammers et al. 2013). Humpback whales are highly migratory, and are most abundant in BC between May and October (Ford et al. 2009). Conversely, there is growing evidence to suggest that fin whales are year-round occupants of the North Pacific (Mizroch et al. 2009, Nichol & Ford 2012). So, not only are fin whales more vulnerable on average to lethal ship strikes (given the higher

[2] Lawson, J., and Lesage, V. Unpublished report. Modelling Ship Strike Risks for Marine Mammals and Sea Turtles. CSAS Working Paper.

speeds of offshore shipping traffic transiting their habitat), but they are also likely exposed to this risk at all times of the year in the study area. In addition to seasonal differences in abundance, there may also be daily or seasonal shifts in whale behaviour (e.g., increased feeding effort) that can change their vulnerability to ship strikes (Panigada et al. 2006). Although our models compared four years of whale survey data (2012-2015) to a single year (2013) of vessel data, the inshore distribution of humpbacks and offshore distribution of fin whales remained consistent across years. For this reason, we are confident that combining the four years of whale sightings data did not obscure any important trends in whale distribution.

Our estimates of future ship strike risk are conservative and are likely under-estimates because we have not accounted for increasing whale densities due to population growth. Humpback population growth rates have been estimated at 4.1% annually in British Columbia (DFO 2009), 6.8% in the entire North Pacific (Calambokidis et al. 2008b) and 6.6% in Western Alaska (Zerbini et al. 2006). Annual rates of increase for fin whales in Western Alaska are estimated at 3.6% (Zerbini et al. 2006). If we assume a constant growth rate of 5% annually, populations of humpback and fin whales off the west coast of Vancouver Island would be expected to double within about 14 years, which would further increase the relative risk of lethal collisions beyond that estimated as a result of increased maritime traffic. We also did not account for increased future lethality as a result of changes to ship size. Cargo and container ship size has doubled since 2000 (Simard et al. 2014), and is expected to continue to grow (Herbert Engineering Corp. and Environmental Research Consulting 2014). Increases to the average draft and beam of larger ocean-going vessels would likely increase the relative incidence of ship strikes. To improve future models, we could quantify and incorporate vessel-specific characteristics that are likely to influence relative strike risk and lethality, such as vessel size, relative noise output, type of propulsion system, vessel manoeuvrability, and bow shape (Lawson & Lesage, *unpub*). Although changes in the routing of international maritime traffic are not anticipated in our study area, growing whale populations could shift relative to their current distributions, which may have unforeseen impacts on the areas where whales are most susceptible to ship strike risk in the future. Overall, it is reasonable to expect that the risk of lethal ship strikes will increase in the study area as a result of greater traffic, larger ship sizes, and growing whale populations.

The most commonly used and effective ship strike mitigation strategies generally fall into two categories: speed limits for ships transiting areas with high whale densities to reduce both the rate and lethality of collisions (e.g., Wiley et al. 2011, McKenna et al. 2012, Conn & Silber 2013), or diverting traffic to avoid such areas entirely and thus reduce the co-occurrence of ships and whales (Vanderlaan & Taggart 2009). Traffic Separation Schemes (TSS) that intersect important whale habitat can also be repositioned to help prevent ship strikes (Silber et al. 2012). For instance, Vanderlaan et al. (2008) estimated that lethal collision risk to right whales in the Bay of Fundy could be reduced by 62% by modifying the location of existing shipping lanes. Other conservation strategies that have been implemented to reduce ship strikes include Passive Acoustic Monitoring (PAM) buoys or bottom-mounted arrays, which detect whale vocalizations in near real-time and broadcast alerts using vessel communication technologies such as AIS or Navigational Telex (NAVTEX) (Clark et al. 2007, Van Parijs et al. 2009, Morano et al. 2012, Reimer et al. 2016) and mandatory VHF marine radio reporting systems (Ward-Geiger et al. 2005, Brown et al. 2007, Silber et al. 2012). Both these approaches serve to warn mariners entering areas with high whale densities. Autonomous underwater vehicles (AUVs, or ocean gliders) have also been suggested as a tool for reporting real-time acoustic detections of whales to vessel operators (Baumgartner et al. 2013). Placing dedicated whale observers onboard vessels might also reduce strike risk by increasing the likelihood that whales are detected in time for the ship's crew to take evasive actions. Active acoustic alarms intended to warn whales of approaching vessels have been tested but were unsuccessful, as these sounds caused diving right whales to return to the surface, which increased their exposure to ship strikes rather than reducing it (Nowacek et al. 2004).

CONCLUSIONS & FUTURE RESEARCH

Ship strike risk analysis based on spatial models of whale density provided a good approach for identifying regions of conservation concern, particularly in areas (e.g., offshore) where actual mortality rates are difficult to quantify from carcass evidence or eye-witness reports. We found evidence of habitat partitioning between humpback and fin whales, with humpback densities being highest on the continental shelf (particularly over the shelf break), and fin whales being distributed at somewhat lower densities offshore of the shelf break. Whales had the potential to be struck by ships in any location where their distributions overlapped with that of marine traffic. In regions of both high whale densities and high intensity marine traffic (e.g., the western portion of Juan de Fuca Strait and the region due west of its entrance), whales were susceptible to elevated risk of lethal ship strikes.

Ship traffic is expected to increase in the future as a result of port expansions in both British Columbia and Washington State. Projections of these increases in the ship strike risk models indicate that the risk of both ship strikes and lethality will increase in the future. Our estimates of increased risk are likely modest, as they do not account for whale population growth or predicted increases in ship length, width or draft. Additional aerial surveys off the west coast of Vancouver Island could be used to further refine our whale density models and ship strike risk estimates – for instance, more surveys might allow for analysis of seasonal or annual trends, or predictions for less frequently encountered species (e.g., blue whales). Future work could also include developing availability and detection bias correction factors to improve the GAM density estimates for humpbacks and fin whales. The models we have developed for predicting the spatial distribution of vulnerable whale populations could be used to advise mariners about high-risk locations for ship-whale collisions. Ultimately, mitigation efforts to reduce the impact of ship strikes on whale populations could include speed restriction zones, areas to be avoided, or PAM-linked mariner notification systems (or a combination of these strategies). In addition, the modelled relative risk of lethal collisions could inform managers about the potential impact of ship strikes on humpback and fin whale populations off the west coast of Vancouver Island.

ACKNOWLEDGEMENTS

We are grateful to the pilots, navigational officers and support staff of Transport Canada's National Aerial Surveillance Program (NASP) and Environment Canada's Marine Aerial Reconnaissance Team (MART), whose expertise and enthusiasm ensured the success of our aerial surveys for cetaceans. We would also like to thank the following individuals for their assistance during the aerial surveys as observers and/or for conducting data entry: Robin Abernethy, Graeme Ellis, Brian Gisborne, James Pilkington, Frances Robertson, Hawsun Sohn, Lisa Spaven, Eva Stredulinsky, and Jared Towers. We thank Christie McMillan for her help in preparing the aerial survey data for spatial analysis. Allan Roberts generously provided code and advice for developing the GAMs in R. Yvan Simard and Nathalie Roy made their 2013 AIS marine traffic data set available for this study and offered guidance in its use. Angelia Vanderlaan and Robert Kenney gave their advice regarding analytical techniques for evaluating ship strike risk. Thomas Doniol-Valcroze provided recommendations regarding the construction and application of detection functions for large whales. Since its inception in 2011, funding for this project (both financial and in-kind) has been provided by the InterDepartmental Recovery Fund, Transport Canada (NASP), Fisheries and Oceans Canada's Species at Risk Program and Strategic Program for Ecosystem-Based Research and Advice, and Port Metro Vancouver.

REFERENCES CITED

Acevedo-Guitierrez, A., Croll, D. A., and Tershy, B. R. 2002. High feeding costs limit dive time in the largest whales. J. Exp. Biol. 205:1747-1753.

Allison, P. A., Smith, C. R., Kukert, H., Deming, J.W., and Bennett, B. A. 1991. Deep-water taphonomy of vertebrate carcasses; a whale skeleton in the bathyal Santa Catalina Basin. Paleobiology 17:78-89.

Barrie, J. V., Hetherington, R., and MacLeod, R. 2014. Pacific margin, Canada shelf physiography: a complex history of glaciation, tectonism, oceanography and sea-level change. *In* Continental Shelves of the World: Their Evolution During the Last Glacio-Eustatic Cycle. Edited by F. L. Chiocci and A. R. Chivas. The Geological Society Memoir No. 41. The Geological Society, Bath, UK. pp. 305-314.

Baumgartner, M.F., Fratantoni, D.M., Hurst, T.P., Brown, M.W., Cole, T.V.N., Van Parijs, S.M., and Johnson, M. 2013. Real-time reporting of baleen whale passive acoustic detections from ocean gliders. J. Acoust. Soc. Am. 134:1814-1823.

Beyer, H. L. 2012. Geospatial Modelling Environment. Version 0.7.3. (Accessed October 12, 2016)

Bezamat, C., Wedekin, L., and Simoes-Lopes, P. 2014. Potential ship strikes and density of Humpback Whales in the Abrolhos Bank breeding ground, Brazil. Aquat. Conserv. Mar. Freshw. Ecosys. 25:712-725.

Brown, M. W., Kraus, S.C., Slay, C. K., and Garrision, L. P. 2007. Survey for discovery, science and management. *In* The Urban Whale: North Atlantic Right Whales at the Crossroads. Edited by S. D. Kraus and R. M. Roland. Harvard University Press, Cambridge, MA. pp 105-137.

Buckland, S. T., Anderson, D. R., Burnham, K. P., Laake, J. L., Borchers, D. L., and Thomas, L. 2001. Introduction to Distance Sampling: Estimating Abundance of Biological Populations. Oxford University Press, Oxford, UK. 448 p.

Calambokidis, J., Schorr, G. S., Steiger, G. H., Francis, J., Bakhtiari, M., Marshall, G., Oleson, E. M., Gendron, D., and Robertson, K. 2008a. Insights into the underwater diving, feeding and calling behavior of blue whales from a suction-cup-attached video-imaging tag (Crittercam). Mar. Tech. Soc. J. 41:19-29.

Calambokidis, J., Falcone, E., Quinn, T. J., Burdin, A. M., Clapham, P. J., Ford, J. K. B., Gabriele, C. M., LeDuc, R., Mattila, D., Rojas-Bracho L., Straley, J. M., Taylor, B. L., Urban R., J., Weller, D., Witteveen, B. H., Yamaguchi, M., Bendlin, A., Camacho, D., Flynn, K., Havron, A., Huggins, J., and Maloney, N. 2008b. SPLASH: Structure of Populations, Levels of Abundance and Status of Humpback Whales in the North Pacific. Final Report for Contract AB133F-03-RP-00078. *Prepared by* Cascadia Research, Olympia, WA *for* the U.S. Dept. of Commerce, Western Administrative Center, Seattle, WA. 57 p.

Campbell, G. S., Thomas, L., Whitaker, K., Douglas, A. B., Calambokidis, J., and Hildebrand, J. A. 2015. Inter-annual and seasonal trends in cetacean distribution, density and abundance off southern California. Deep-Sea Res. II 112:143-157.

Chamberlain, A. 2015. 'Extremely rare sighting' of Fin Whale in waters off Vancouver Island. Times Colonist. September 5, 2015 edition. Victoria, BC.

Clark, C. W., Gillespie, D., Nowacek, D. P., and Parks, S. E. 2007. Listening to their world: acoustics for monitoring and protecting right whales in an urbanized ocean. *In* The Urban Whale: North Atlantic Right Whales at the Crossroads. Edited by S. D. Kraus and R. M. Rolland. Harvard University Press, Cambridge, MA. pp. 333-357.

Conn, P. B., and Silber, G. K. 2013. Vessel speed restrictions reduce risk of collision-related mortality for North Atlantic right whales. Ecosphere 4:1-15.

Constantine, R., Johnson, M., Riekkola, L., Jervis, S., Kozmian-Ledward, L., Dennis, T., Torres, L. G., and Aguilar de Soto, N. 2015. Mitigation of vessel-strike mortality of endangered Bryde's whales in the Hauraki Gulf, New Zealand. Biol. Conserv. 186:149-157.

COSEWIC. 2015. Committee on the Status of Endangered Wildlife in Canada. (Accessed October 12, 2016)

Croll, D. A., Tershy, B. R., Hewitt, R. P., Demer, D. A., Fiedler, P. C., Smith, S. E., Armstrong, W., Popp, J. M., Kiekhefer, T., Lopez, V. R., Urban, J., and Gendron, D. 1998. An integrated approach to the foraging ecology of marine birds and mammals. Deep-Sea Res. II 45:1353-1371.

Croxall, J. P., Everson, I., Kooyman, G. L., Ricketts, C., and Davis, R. W. 1985. Fur seal diving behavior in relation to krill vertical distribution. J. Anim. Ecol. 54:1-8.

Dalla Rosa, L., Ford, J. K. B., and Trites, A. W. 2012. Distribution and relative abundance of humpback whales in relation to environmental variables in coastal British Columbia and adjacent waters. Continental Shelf Res. 36:89-104.

DFO. 2009. Recovery potential assessment of humpback whales, Pacific population. DFO Can. Sci. Advis. Sec. Sci. Advis. Rep. 2009/048.

Dransfield, A., Hines, E., Mcgowan, J., Holzman, B., Nur, N., Elliott, M., Howar, J., and Jahncke, J. 2014. Where the whales are: using habitat modeling to support changes in shipping regulations within National Marine Sanctuaries in Central California. Endang. Species Res. 26:39-57.

ESRI. 2013. ArcGIS Desktop: Education Edition. Version 10.2. Environmental Systems Research Institute (ESRI), Redlands, CA.

Fisheries and Oceans Canada. 2013a. Partial Action Plan for Blue, Fin, Sei and North Pacific Right Whales (*Balaenoptera musculus, B. physalus, B. borealis,* and *Eubalaena japonica*) in Pacific Canadian Waters. *Species at Risk Act* Action Plan Series. Fisheries and Oceans Canada, Ottawa. iv + 23 pp.

Fisheries and Oceans Canada. 2013b. Recovery Strategy for the North Pacific Humpback Whale (*Megaptera novaeangliae*) in Canada. *Species at Risk Act* Recovery Strategy Series. Fisheries and Oceans Canada, Ottawa. x + 67 pp.

Flinn, R. D., Trites, A. W., Gregr, E. J., and Perry, R. I. 2002. Diets of fin, sei, and sperm whales in British Columbia: An analysis of commercial whaling records, 1963-1967. Mar. Mamm. Sci. 18:663-679.

Forcada, J., Aguilar, A., Hammond, P., Pastor, X., and Aguilar, R. 1996. Distribution and abundance of Fin Whales (*Balaenoptera physalus*) in the western Mediterranean sea during the summer. J. Zool. Soc. London 238:23-34.

Ford, J. K. B. 2014. Marine Mammals of British Columbia. Royal BC Museum, Victoria, BC. 460 p.

Ford, J. K. B., Abernethy, R. M., Phillips, A. V., Calambokidis, J., Ellis, G. M., and Nichol, L. M. 2010. Distribution and Relative Abundance of Cetaceans in Western Canadian Waters from Ship Surveys, 2002-2008. Can. Tech. Rep. Fish. Aquat. Sci. 2913. v + 51 p.

Ford, J. K. B., Rambeau, A. L., Abernethy, R. M., Boogaards, M. D., Nichol, L. M., and Spaven, L. D. 2009. An Assessment of the Potential for Revovery of Humpback Whales off the Pacific Coast of Canada. DFO Can. Sci. Advis. Sec. Res. Doc. 2009/015. iv + 33 p.

Friends of the San Juan Islands and San Juan Islanders for Safer Shipping. 2015. Salish Sea Vessel Traffic Projections: New and Expanding Terminals and Refinery. 11 p.

Gannier, A. 2006. Le peuplement estival de cétacés dans le Sanctuaire Marin PELAGOS (Méditerranée nord-occidentale) : distribution et abondance. Mammalia 70:17-27.

Goldbogen, J. A., Calambokidis, J., Shadwick, R. E., Oleson, E. M., Mcdonald, M. A., and Hildebrand, J. A. 2006. Kinematics of foraging dives and lunge-feeding in Fin Whales. J. Exp. Biol. 209:1231-1244.

Gregr, E. J., and Trites, A. W. 2001. Predictions of critical habitat for five whale species in the waters of coastal British Columbia. Can. J. Fish. Aquat. Sci. 58:1265-1285.

Harris, K. S., Gende, M., Logsdon, M. G., and Klinger, T. 2012. Spatial pattern analysis of cruise ship-humpback whale interactions in and near Glacier Bay National Park, Alaska. Environ. Manage. 49:44-54.

Herbert Engineering Corp. and Environmental Research Consulting. 2014. Roberts Bank Terminal 2 Technical Report: Marine Vessel Incidence Prediction Inputs to the Quantitative Risk Assessment. File: 2013-032-01 Rev. 2. *Prepared for* Port Metro Vancouver, Vancouver, BC. 269 p.

Kim, Y. J., and Gu, C. 2004. Smoothing spline Gaussian regression: more scalable computation via efficient approximation. J. R. Stat. Soc. Ser. B 66:337-356.

Kot, B. W., Sears, R., Zbinden, D., Borda, E., and Gordon, M. S. 2014. Rorqual whale (Balaenopteridae) surface lunge-feeding behaviors: Standardized classification, repertoire diversity, and evolutionary analyses. Mar. Mamm. Sci. 30:1335-1357.

Laist, D. W., Knowlton, A. R., Mead, J. G., Collet, A. S., and Podesta, M. 2001. Collisions between ships and whales. Mar. Mamm. Sci. 17:35-75.

Lammers, M. O., Pack, A. A., Lyman, E. G., and Espiritu, L. 2013. Trends in collisions between vessels and North Pacific humpback whales (*Megaptera novaeangliae*) in Hawaiian waters (1975-2011). J. Cetacean Res. Manage. 13:73-80.

McKenna, M. F., Calambokidis, J., Oleson, E. M., and Goldbogen, J. A. 2015. Simultaneous tracking of blue whales and large ships demonstrated limited behavioural responses for avoiding collision. Endang. Spec. Res. 27:219-232.

McKenna, M. F., Katz, S. L., Condit, C., and Walbridge, S. 2012. Response of commercial ships to a voluntary speed reduction measure: Are voluntary strategies adequate for mitigating ship-strike risk? Coast. Manage. 40:634-650.

Miller, D. L. 2016. Distance: Distance Sampling Detection Function and Abundance Estimation. R Package Version 0.9.6.

Mizroch, S. A., Rice, D. W., Zwiefelhofer, D., Waite, J., and Perryman, W. L. 2009. Distribution and movements of Fin Whales in the North Pacific Ocean. Mamm. Rev. 39:193-227.

Morano, J.L., Rice, A.N., Tielens, J.T., Estabrook, B.J., Murray, A., Roberts, B.L., and Clark, C.W. 2012. Acoustically detected year-round presence of right whales in an urbanized migration corridor. Conserv. Biol. 26(4):698-707.

Nichol, L. M. and Ford, J. K. B. 2012. Information Relevant to the Assessment of Critical Habitat for Blue, Fin, Sei and North Pacific Right Whales in British Columbia. DFO Can. Sci. Advis. Sec. Res. Doc. 2011/137. vi + 31 p.

Nowacek, D. P., Friedlaender, A. S., Halpin, P. N., Hazen, E. L., Johnston, D. W., Read, A. J., Espinasse, B., Zhou, M., and Zhu, Y. 2011. Super-aggregations of krill and humpback whales in Wilhemina Bay, Antarctic Peninsula. PLoS ONE 6(4): e19173.

Nowacek, D. P., Johnson, M. P., and Tyack, P. L. 2004. North Atlantic right whales (*Eubalaena glacialis*) ignore ships but respond to alerting stimuli. Proc. R. Soc. B 271:227-231.

Nuka Research & Planning Group, LLC. 2013. West Coast Spill Response Study. Volume 2: Vessel Traffic Study. *Prepared for* the British Columbia Ministry of the Environment. 106 p.

Oleson, E. M., Calambokidis, J., Burgess, W. C., McDonald, M. A., LeDuc, C. A., and Hildebrand, J. A. 2007. Behavioral context of call production by eastern North Pacific blue whales. Mar. Ecol. Prog. Ser. 330:269-284.

Panigada, S., Pesante, G., Zanardelli, M., Capoulade, F., Gannier, A., and Weinrich, M. T. 2006. Mediterranean Fin Whales at risk from fatal ship strikes. Mar. Pollut. Bull. 52:1287-1298.

Panigada, S., Zanardelli, M., Mackenzie, M., Donovan, C., Melin, F., and Hammond, P. S. 2008. Modelling habitat preferences for Fin Whales and striped dolphins in the Pelagos Sanctuary (Western Mediterranean Sea) with physiographic and remote sensing variables. Remote Sens. Environ. 112:3400-3412.

Pebesma, E. J. 2004. Multivariable geostatistics in S: the gstat package. Comp. Geosci. 30:683-691.

Perry, M. J., Bolger, J. P., and English, D. C. 1989. Primary production in Washington coastal waters. *In* Coastal Oceanography of Washington and Oregon. Edited by M. R. Landry and B. M. Hickey. Elsevier, Amsterdam. pp. 117-138.

Reimer, J., Gravel, C., Brown, M.W., and Taggart, C.T. 2016. Mitigating vessel strikes: The problem of the peripatetic whales and the peripatetic fleet. Marine Policy 68:91-99.

Schnute, J. T., Boers, N., and Haigh, R. 2015. PBSmapping: Mapping Fisheries Data and Spatial Analysis Tools. R package Version 2.69.76

Silber, G. K., Slutsky, J., and Bettridge, S. 2010. Hydrodynamics of a ship/whale collision. J. Exp. Mar. Biol. Ecol. 391:10-19.

Silber, G. K., Vanderlaan, A. S. M., Tejedor Arceredillo, A., Johnson, L., Taggart, C. T., Brown, M. W., Bettridge, S., and Sagarminaga, R. 2012. The role of the International Maritime Organization in reducing vessel threat to whales: Process, options, action and effectiveness. Mar. Policy 36:1221-1233.

Simard, Y., Roy, N., Giard, S., and Yayla, M. 2014. Canadian Year-round Shipping Traffic Atlas for 2013: Volume 3, West Coast. Can. Tech. Rep. Fish. Aquat. Sci. 3091. xviii + 327 p.

Thomas, L., Buckland, S. T., Burnham, K. P., Anderson, D. R., Laake, J. L., Borchers, D. L., and Strindberg, S. 2002. Distance Sampling. *In* Encyclopedia of Environmetrics. Edited by A. H. El-Shaarawai and W. W. Piegorsch. John Wiley & Sons, Ltd, Chichester, UK. pp. 544-552.

Van Parijs, S. M., Clark, C. W., Sousa-Lima, R. S., Parks, S. E., Rankin, S., Risch, D., and Van Opzeeland, I. C. 2009. Management and research applications of real-time and archival passive acoustic sensors over varying temporal and spatial scales. Mar. Ecol. Prog. Ser. 395:21-36.

Vanderlaan, A. S. M., and Taggart, C. T. 2007. Vessel collisions with whales: the probability of lethal injury based on vessel speed. Mar. Mamm. Sci. 23:144-156.

Vanderlaan, A. S. M., and Taggart, C. T. 2009. Efficacy of a voluntary area to be avoided to reduce risk of lethal vessel strikes to endangered whales. Conserv. Biol. 23:1467-1474.

Vanderlaan, A. S. M., Taggart, T., Serdynska, A. R., Kenney, A. R., and Brown, M. W. 2008. Reducing the risk of lethal encounters: vessels and right whales in the Bay of Fundy and on the Scotian Shelf. Endang. Species Res. 4:283-297.

Wade, P. 1998. Calculating limits to the allowable human-caused mortality of cetaceans and pinnipeds. Mar. Mamm. Sci. 14:1-37.

Ward-Geiger, L. I., Silber, G. K., Baumstark, R. D., and Pulfer, T. L. 2005. Characterization of ship traffic in right whale critical habitat. Coast. Manage. 33:263-278.

Ware, D. M., and Thomson, R. E. 2005. Bottom-up ecosystem trophic dynamics determine fish production in the Northeast Pacific. Science 308:1280-1284.

Webb, K. R., and Gende, S. M. 2015. Activity patterns and speeds of large cruise ships in Southeast Alaska. Coastal Manage. 43:67-83.

Wiley, D. N., Thompson, M., Pace, R. M. I., and Levenson, J. 2011. Modeling speed restrictions to mitigate lethal collisions between ships and whales in the Stellwagen Bank National Marine Sanctuary, USA. Biol. Conserv. 144:2377-2381.

Williams, R., and O'Hara, P. 2009. Modelling ship strike risk to fin, humpback and killer whales in British Columbia, Canada. J. Cetacean Res. Manage. 11:1-10.

Wood, S. N. 2006. Generalized Additive Models: An Introduction with R. Chapman & Hall/CRC.

Wood, S. N. 2004. Stable and efficient multiple smoothing parameter estimation for generalized additive models. J. Am. Stat. Assoc. 99:673-686.

Wood, S. N. 2011. Fast stable restricted maximum likelihood and marginal likelihood estimation of semiparametric generalized linear models. J. R. Stat. Soc. B 73:3-36.

Zerbini, A. N., Waite, J. M., Laake, J. L., and Wade, P. R. 2006. Abundance, trends and distribution of baleen whales off Western Alaska and the central Aleutian Islands. Deep-Sea Res. I 53:1172-1790.

Zuur, A. F., Ieno, E. N., and Elphick, C. S. 2010. A protocol for data exploration to avoid common statistical problems. Methods Ecol. Evol. 1:3-14.

Zuur, A. F., Ieno, E. N., Walker, N. J., Saveliev, A. A., and Smith, G. M. 2009. Mixed Effects Models and Extensions in Ecology with R. Springer Science+Business Media, New York, NY. 574 p.

TABLES

Table 1. Summary of vessel speed categories and associated median speeds (knots), 2013 AIS ship traffic data set.

Vessel speed class (knots)	Median speed (knots)
5-10	7.5
10-15	12.5
15-20	17.5
> 20	23

Table 2. Summary by species of the number of baleen whales detected on 34 aerial surveys (2012-2015) off the west coast of Vancouver Island, British Columbia, Canada. Sightings that occurred during unfavourable environmental conditions (Beaufort wind force >4, visibility ≤5 nm), at altitudes > 366 m, or during “OFF” or “ONC” effort segments of survey track were excluded.

Species	No. of sightings	No. of individuals
Humpback whale, *Megaptera novaeangliae*	141	305
Fin whale, *Balaenoptera physalus*	54	89
Blue whale, *Balaenoptera musculus*	3	3
Minke whale, *Balaenoptera acutorostrata*	1	1
Grey whale, *Eschrichtius robustus*	5	9
‘Like humpback whale’	19	25
‘Like fin whale’	20	31
‘Like grey whale’	1	1
‘Unidentified large baleen whale’	4	6
‘Unidentified large whale’	28	33
TOTAL	276	503

Table 3. Candidate models for predicting densities of humpback and fin whales off the west coast of Vancouver Island, BC (2012-2015). All models included the offset term of logged aggregate effort area (km^2) per grid cell. W_i indicates model weights, with the final selected model starred (*). Where candidate models had AIC values differing by <2, the simpler model was chosen.

	Candidate GAMs	AIC	ΔAIC	W_i
Humpback Whales	$N \sim s(\sqrt{\lvert depth \rvert}) + s(UTM\ northing) + slope$	841.464	0	0.580
	$N \sim s(\sqrt{\lvert depth \rvert}) + s(UTM\ northing)$	842.111	0.647	0.420*
	$N \sim 1$	1063.741	222.277	0
Fin Whales	$N \sim s(\sqrt{\lvert depth \rvert})$	668.952	0	0.754
	$N \sim s(\sqrt{\lvert depth \rvert}) + s(UTM\ northing) + slope$	671.191	2.239	0.246
	$N \sim 1$	693.255	24.303	0

Table 4. Negative binomial GAM (log link function) results of top-ranked model for humpback whale counts (N=159 sightings, 329 individuals; 'humpback whale' & 'like humpback whale') over the 25 km^2 gridded study area off the west coast of Vancouver Island, BC, Canada, with significant relationships starred (*).

Output parameters	Coefficients of top-ranked GAM		
	Intercept	s(UTM northing)	s(sqrt(Depth))
Estimate	-7.087	—	—
standard error	0.314	—	—
z-value	-22.58	—	—
edf	—	4.062	4.731
Ref.df	—	5.060	5.745
Chi.sq	—	11.9	131.7
p-value	<0.001*	0.038*	<0.001*
R^2 (adjusted)	0.136	—	—
-REML score	423.46	—	—
Deviance explained	66.1%	—	—
AIC	842.111	—	—

Table 5. Negative binomial GAM (log link function) results of top-ranked model for fin whale counts (N=74 sightings, 120 individuals; 'fin whale' & 'like fin whale') over the 25 km^2 gridded study area off the west coast of Vancouver Island, BC, Canada, with significant relationships starred (*).

Output parameters	Coefficients of top-ranked GAM	
	Intercept	s(sqrt(Depth))
Estimate	-6.334	—
standard error	0.242	—
z-value	-26.21	—
Edf	—	2.688
Ref.df	—	3.32
Chi.sq	—	16.69
p-value	<0.001*	0.0013*
R^2 (adjusted)	0.022	—
-REML score	332.99	—
Deviance explained	26.7%	—
AIC	668.952	—

Table 6. Projected changes in shipping traffic (number of vessels) transiting the Strait of Juan de Fuca and southern Strait of Georgia, by ship type, between 2012 and 2030. The future predicted number of ships for 2030 includes the current fleet of ships operating in these areas, as well additional ships predicted in the Herbert Engineering Corp. and Environmental Research Consulting (2014) report for Roberts Bank Terminal 2 expansion. Future increases in the number of vessels bound for Puget Sound ports are likely under-represented in this 2030 prediction. Proportional changes in the number of ships that were applied as multipliers to the corresponding speed classes from the 2013 AIS shipping data set are starred (*).

Speed	Ship type	2012	2030	Proportional change
10-15 knots	Container	521	503	0.97
	Bulk carrier	882	1059	1.20
	General cargo	262	239	0.91
	Chemical carrier	161	265	1.65
	Total (10-15 knots)	1826	2066	1.13*
15-20 knots	Tanker	74	427	5.77
	Cruise ship	190	190	1.00
	Total (15-20 knots)	264	617	2.34*
	TOTAL (all ships)	2090	2683	1.28

Table 7. Projected number of ship transits in the Salish Sea in 2015 and in the future based on current expansions and proposed developments. Projections are taken from a report by San Juan Islanders for Safer Shipping; includes data from U.S. waters but does not include cruise ship data. Vessel transits associated with activities primarily restricted to the Strait of Georgia were excluded from these counts. Proportional changes in the number of transits that were applied as multipliers to the corresponding speed classes from the 2013 AIS shipping data set are starred (*).

Ship type	2015	Future	Proportional change
10-15 knots (Container/Bulk/Carrier)	12,274	15,130	1.23*
15-20 knots (Tanker)	120	1576	13.13*
TOTAL (all ships, 10-20 knots)	12,394	16,706	1.35

FIGURES

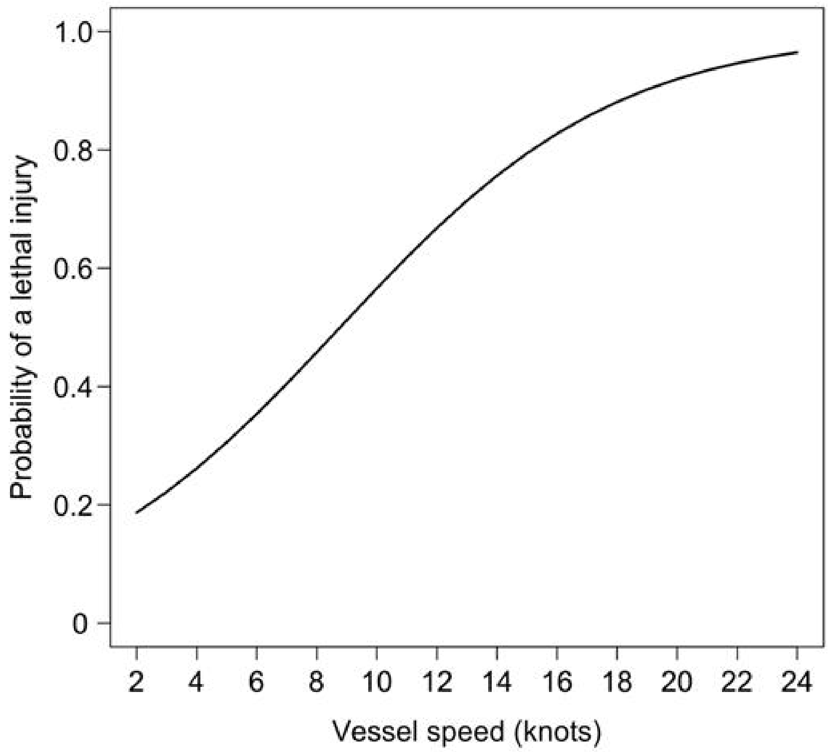

Figure 1. Logistic regression model (from Conn & Silber 2013) showing the probability of lethal injury to a large whale from a vessel strike, as a function of vessel speed (knots).

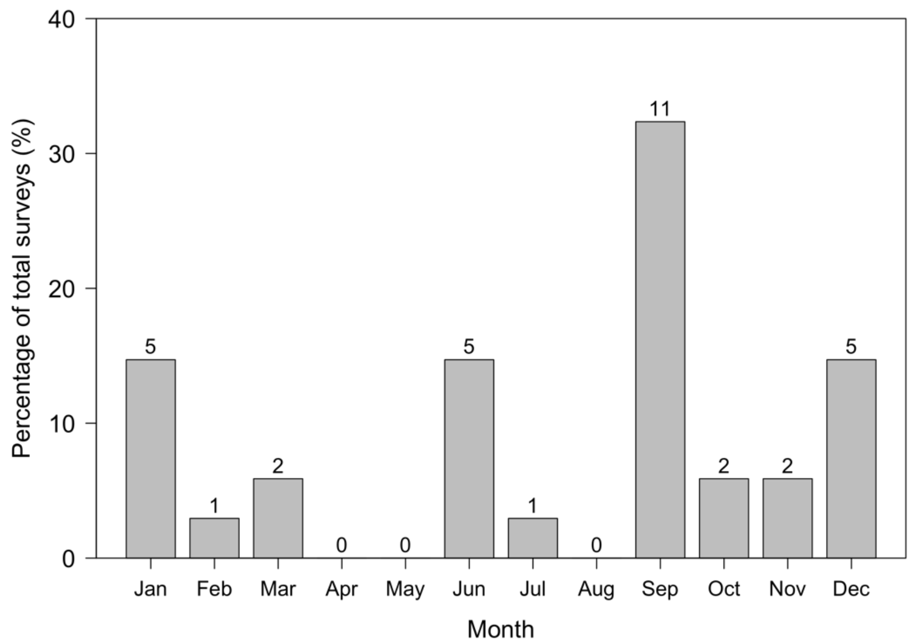

Figure 2. Percentage of whale aerial surveys by month, conducted off the west coast of Vancouver Island (2012-2015). Numbers displayed above the bars indicate the total number of surveys flown in that month.

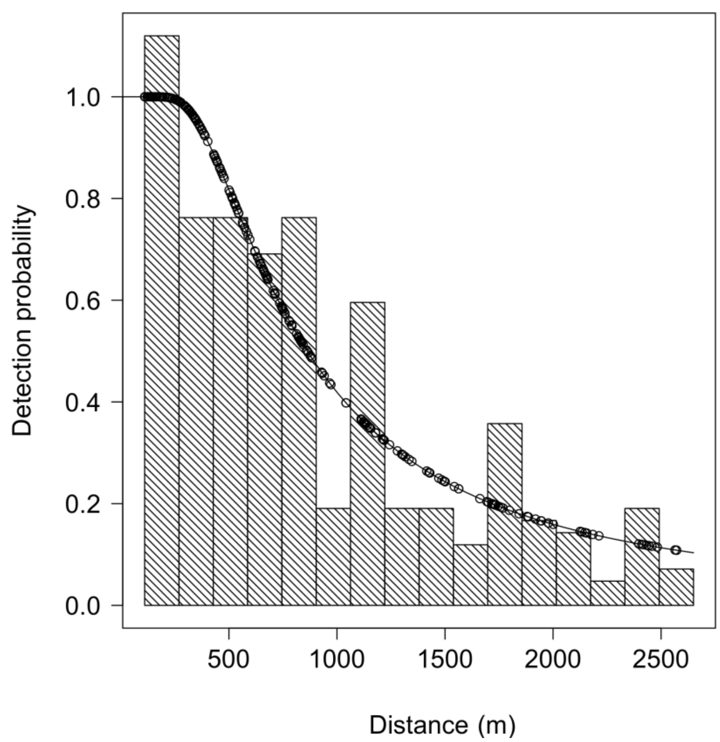

Figure 3. CDS hazard rate detection function (AIC=4054.86, w=2650 m, esw=1010 m, no expansion terms) for large whale sightings (N=267, after truncation) made off the west coast of Vancouver Island, Canada from a Dash-8 aircraft (2012-2015).

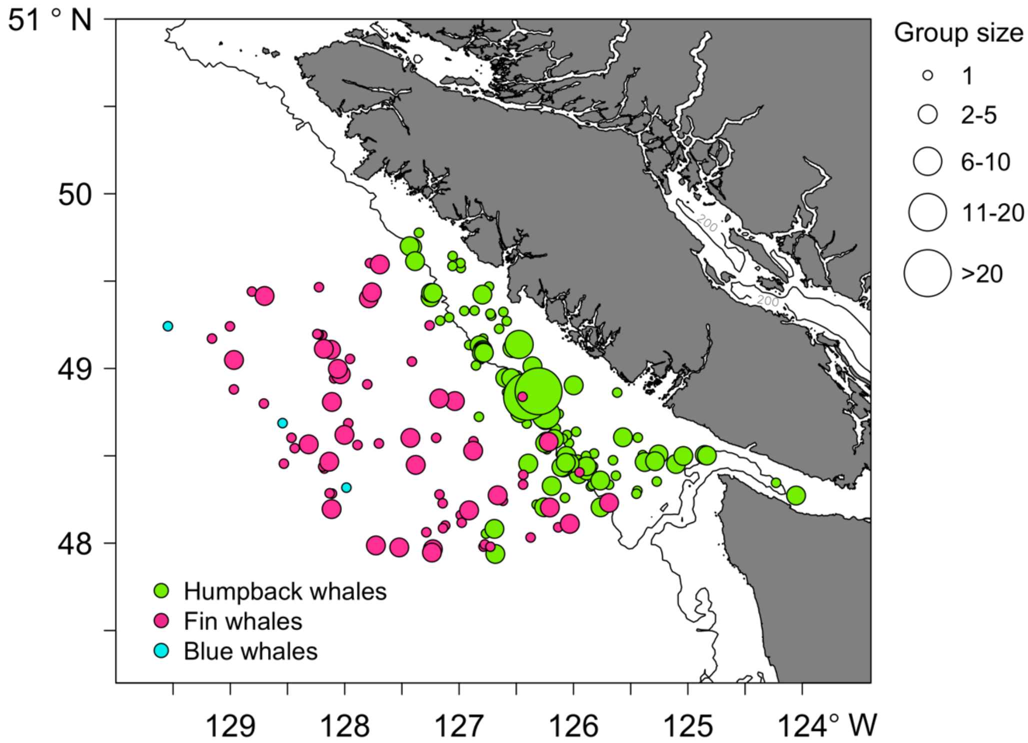

Figure 4. Locations of large whale sightings (N=237) by species and group size (range = 1-33), observed during aerial surveys off the west coast of Vancouver Island and western Juan de Fuca Strait (2012-2015). The continental shelf break is illustrated by the 200 m bathymetric contour (black line).

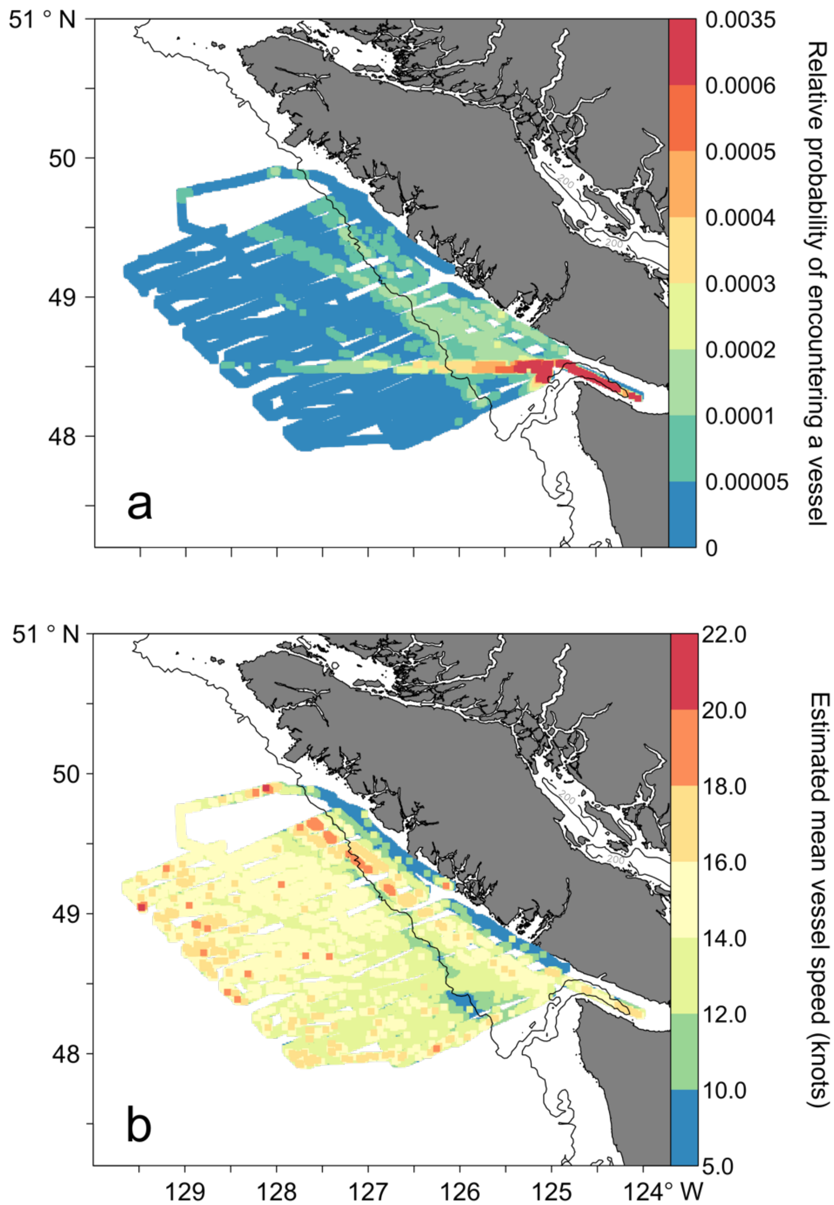

Figure 5. Aerial survey study area off the west coast of Vancouver Island, BC, Canada, divided into 1 km^2 grid cells (N=23,996). Filled cells indicate those containing survey effort that was retained for analysis. Colours indicate (a) the probability of encountering a vessel and (b) the estimated mean vessel speed (knots); 2013 AIS ship traffic data set. The continental shelf break is illustrated by the 200 m bathymetric contour (black line). The colour bar for (a) is scaled similarly to Fig. 7 (c) and (d) to facilitate comparisons. Note that colour bar increments for the lowest and highest categories are not necessarily placed at equivalent intervals, to allow for more detailed visualization of the majority of the data range.

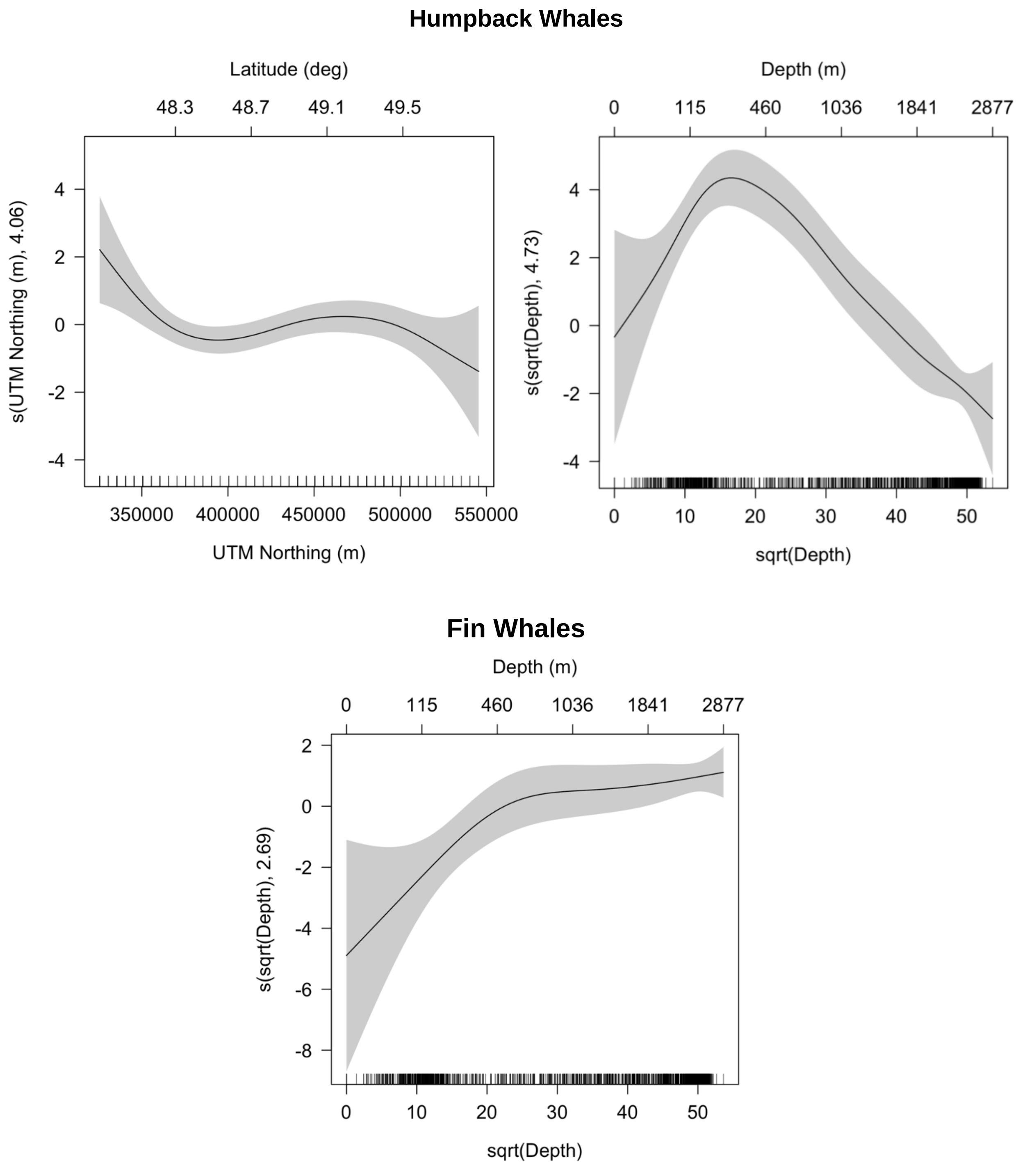

Figure 6. Smoothing functions (solid lines) with 95% confidence intervals (shaded bands) for the explanatory variables, UTM northing (latitude) and depth, of the top-ranked negative binomial GAMs estimating humpback (top panels) and fin (bottom panels) whale densities over a gridded surface of 25 km^2 cells. y-axis labels display the fitted function with the estimated degrees of freedom in parentheses, while x-axis rug plots indicate the distribution of sampled values within each explanatory variable. For ease of interpretation, the latitude smoother includes x-axes showing both projected (UTM, m) and approximate geographic (latitude, deg) values, and the depth smoothers include x-axes showing both square-root transformed (m$^{1/2}$) and untransformed (m) values.

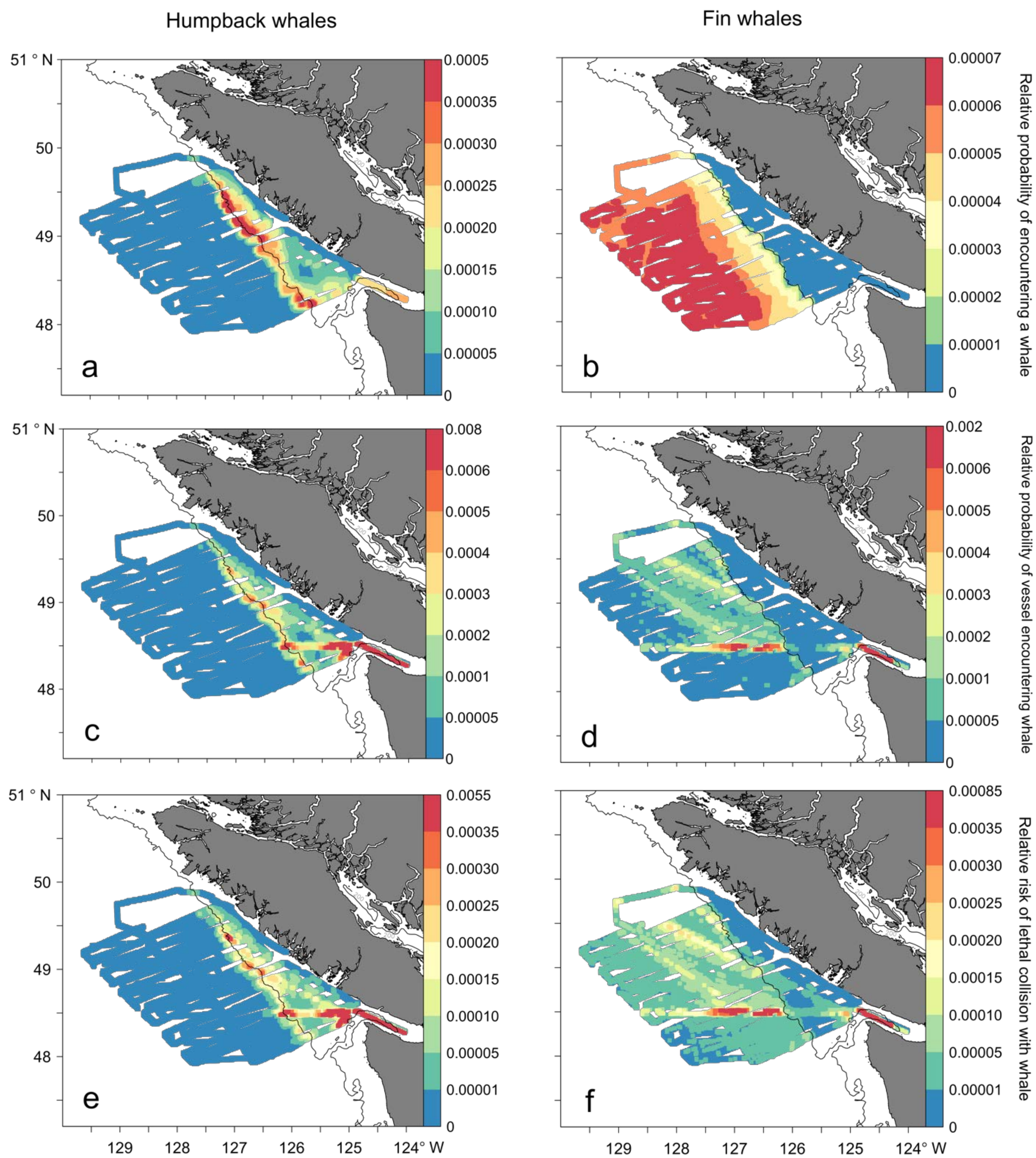

Figure 7. Aerial survey study area off the west coast of Vancouver Island, BC, Canada, divided into 1 km^2 grid cells (N=23,996). Filled cells indicate those containing survey effort that was retained for analysis. Colours indicate the relative probability of (a,b) encountering a humpback or fin whale (calculated from GAM model estimates of whale densities), (c,d) a vessel encountering a humpback or fin whale, and (e,f) the relative risk of a lethal collision between a vessel and a humpback or fin whale; 2013 AIS ship traffic data set. The continental shelf break is illustrated by the 200 m bathymetric contour (black line). Colour bars for (c), (d), and Fig. 5 (a) are scaled similarly to facilitate comparisons, as are colour bars for (e) and (f). Note that colour bar increments for the lowest and/or highest categories are not necessarily placed at equivalent intervals, to allow for more detailed visualization of the majority of the data range.

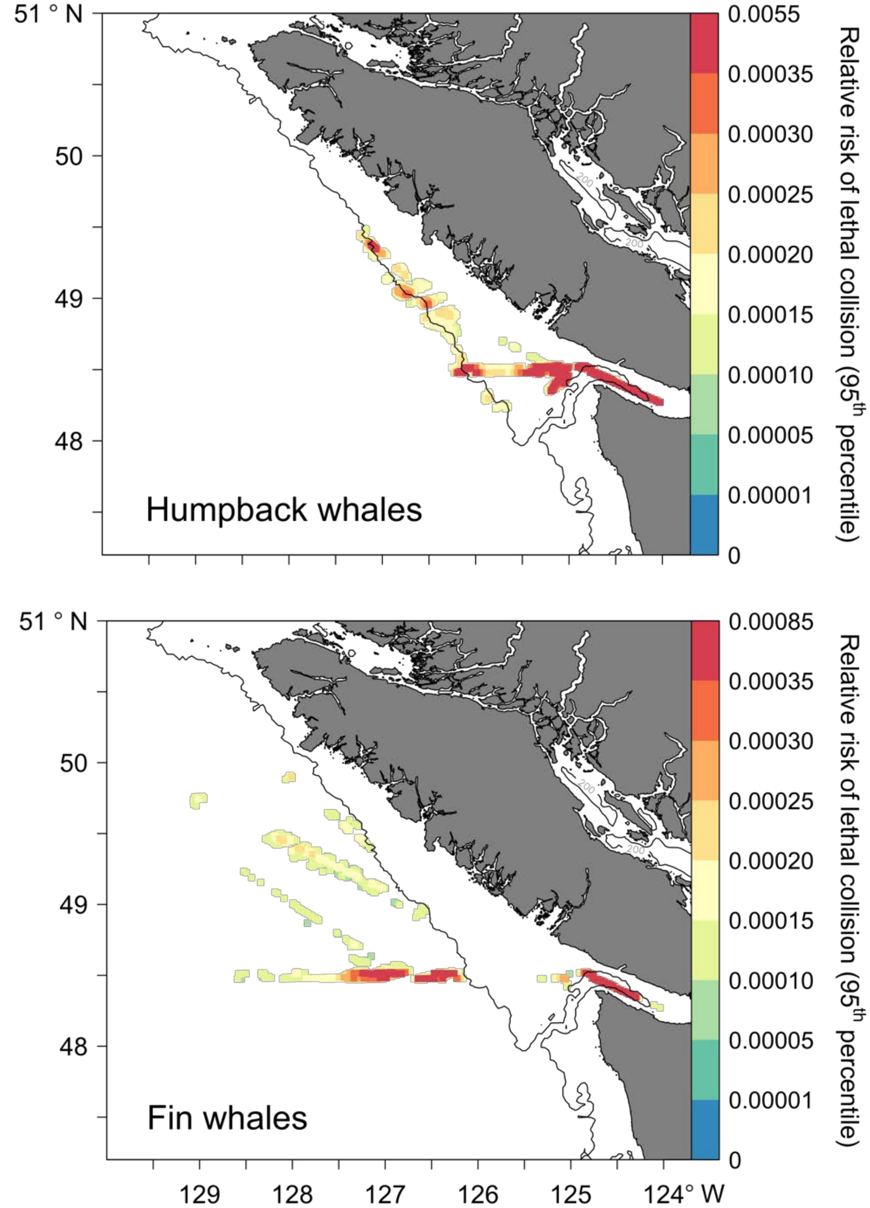

Figure 8. Filled cells (N=1200) indicate the areas of highest relative risk (95th percentile) of lethal collisions (per 1 km^2) between ships and humpback (top) and fin whales (bottom); 2013 AIS ship traffic data set. Mean relative risk of a lethal collision is 35.2-fold higher for humpback whales and 8.1-fold higher for fin whales in the illustrated areas than in the remainder of the surveyed study area. The continental shelf break is indicated by the 200 m bathymetric contour (black line). Colour bars are scaled similarly to one another, and to Fig. 7 (e,f) to facilitate comparisons. Note that colour bar increments for the lowest and/or highest categories are not necessarily placed at equivalent intervals, to allow for more detailed visualization of the majority of the data range.